Technical Report
RAL-TR-96-053

Contributions to EPAC'96

Members of the ISIS Facility

July 1996

COUNCIL FOR THE CENTRAL LABORATORY OF THE RESEARCH COUNCILS

Enquiries about copyright, reproduction and requests for additional copies of this report should be addressed to:

The Central Laboratory of the Research Councils
Library and Information Services
Rutherford Appleton Laboratory
Chilton
Didcot
Oxfordshire
OX11 0QX
Tel: 01235 445384 Fax: 01235 446403
E-mail library@rl.ac.uk

ISSN 1358-6254

RAL Report
RAL-96-053

CONTRIBUTIONS TO

EPAC'96

Sitges, Barcelona

5th EUROPEAN PARTICLE ACCELERATOR CONFERENCE
EUROPHYSICS CONFERENCE
Melia Gran Sitges Hotel, Sitges
10 June - 14 June 1996

BY MEMBERS OF THE ISIS FACILITY

Papers to be published in the EPAC'96 Conference Proceedings

July 1996

Rutherford Appleton Laboratory, Chilton, Didcot, Oxon OX11 0QX

CONTRIBUTIONS TO

EPAC'96

Sitges, Barcelona

5th EUROPEAN PARTICLE ACCELERATOR CONFERENCE
EUROPHYSICS CONFERENCE
Melia Gran Sitges Hotel, Sitges
10 June - 14 June 1996

BY MEMBERS OF THE ISIS FACILITY

D J Adams, T W Aitken[1], C P Bailey, P J S B-Barratt, R G Bendall, J R J Bennett, N Bliss[1], A I Borden, T A Broome, R A Burridge, J A Clarke[1], M A Clarke-Gayther, V C Cloke, C J Densham, P Drumm, J Duke, W R Evans, I S K Gardner, P E Gear, M Glover, M R Harold, M Holding, J Kay[1], A P Letchford, G M McPherson, N Marks[1], G R Martin, S Metcalf[1], W A Morris, G R Murdoch, V Panteleev[3], M Perkins, C W Planner, H Price[1], C R Prior, H Ravn[2], G H Rees OBE, H Schönauer[2], R Sidlow, S Stoneham[4], T G Walker, D D Warner[1], C M Warsop and D Wright

[1] CLRC staff (not from ISIS)
[2] CERN staff
[3] PNPI RAS, Gatchina, Russia
[4] Elgood & Dye Limited

Papers to be published in the EPAC'96 Conference Proceedings

July 1996

CONTENTS

HIGH POWER TARGETS FOR SPALLATION SOURCES

Tim Broome, Rutherford Appleton Laboratory, Chilton, Didcot, Oxon., UK.

ABSTRACT

Spallation, the bombardment of a heavy metal target by an intense beam of protons, has become an established technique for the production of high intensity fluxes of neutrons. There are, currently, proposals and design studies for a variety of high power sources covering an increasing range of applications such as energy production, transmutation of radioactive waste and tritium production facilities as well as the second generation of neutron sources for condensed matter research. Design of the targets for high power spallation sources, with a beam power of several megawatts, presents a formidable technical challenge both in terms of heat removal and materials selection. The requirements and concepts for such targets are reviewed.

1 INTRODUCTION

Public concern over the operational safety of nuclear reactors, together with the problems associated with the long term management of radioactive waste, has made approval of new reactors increasingly difficult.

Considerable efforts have been made to investigate the use of accelerator based systems as an alternative in almost all areas traditionally covered by reactors. In particular these include:

- Thermal neutron beam sources
- Materials irradiation studies
- Isotope production
- Tritium production
- Transmutation of radioactive waste
- Power Generation

At present there are four operational thermal neutron beam sources: KENS KEK Japan 3 kW, IPNS ANL USA 7 kW, MLNSC LANL USA 60 kW and ISIS, RAL UK 160 kW. The SINQ source at PSI in Switzerland is expected to start operation later this year at 1 MW beam power and a 240 kW source is under construction based on the linac at the Moscow Meson Factory. The LANSC linac operates at 1 MW and the complex includes a materials irradiation facility.

Spallation sources generally employ a high intensity proton beam with an energy of, typically, 1 - 2 GeV although there have been proposals to use beam energies up to 10 GeV. All depend on the provision of an efficient target system to produce the high neutron fluxes required. The various uses impose, in detail, different requirements for targets. The main challenge for the target designer is to optimise the useful neutron production within the practical engineering constraints of heat removal and taking account of the radiation damage to the target and structural materials.

2 SPALLATION

The spallation process is illustrated in figure 1. The proton beam is incident on a heavy metal target which is, typically, about one range length long (30 - 60 cm.).

When a proton interacts with a target nucleus a few energetic particles are produced, leaving the nucleus in a highly excited state. The nucleus returns to the ground state by emission of neutrons, protons, deuterons, tritons and alpha particles - 'evaporation'. The energetic particles go on to interact with other target nuclei producing more excited nuclei, and hence neutrons, in a nuclear cascade. The evaporation neutrons, with a typical energy of about 1 MeV, travel through the target material and those which escape from the target form the useful source for the applications listed above.

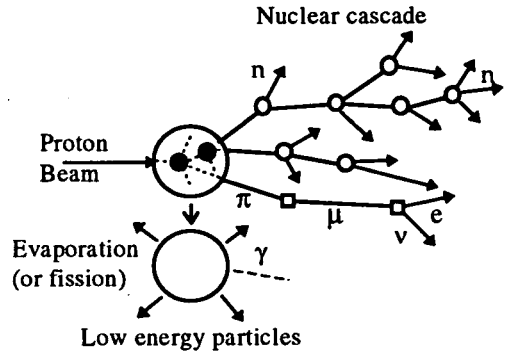

Figure 1. The Spallation Process

In many target materials the excited nuclei will undergo fission to leave two fragments which will de-excite by evaporation.

These processes deposit heat in the target, the majority from ionisation loss of the protons with some from the kinetic energy of the nuclear recoils. For targets where the amount of fission is small about 60% of the proton beam energy is deposited as heat. The heat deposited in a target with significant fission cross section is from 1.5 to many times the beam power, depending on the fission multiplication.

The nuclear interactions also result in damage to the target material and the production of considerable quantities of hydrogen and helium.

Several computer codes have been developed to calculate the complete physics of the spallation process and transport of the secondary particles. The most commonly used being based on the HETC [1] package. These have flexible 3 D geometry packages which allow the inclusion of full engineering details in the calculations.

3 TARGET MATERIALS

For a thick target the dependence of the yield of neutrons per proton as a function of proton beam energy (E GeV) and target material (atomic mass number A) is given by [2]:

$$\text{Yield} = 0.1\,(A+20)\,(E-0.12) \quad (A< 238)$$
$$= 50\,(E-0.120) \quad \text{(Fissionable targets)}$$

The desirable properties of a spallation target material are:

- High Atomic number
- High density
- High/Low melting point (solid/liquid)
- High thermal conductivity
- Chemically inert, low corrosion
- Resistance to radiation damage
- Low resonance integral for neutron absorption
- (Low absorption for thermal neutrons) see section 6
- Good availability and low price

The most important property is high atomic number to maximise the neutron production. The usual materials considered are tungsten and tantalum (and their alloys) for solid targets. Liquid metals considered have been lead, lead/bismuth eutectic and, more recently, mercury.

The advantage of a fissionable material is clear in this respect. To date targets made from uranium have been operated at KENS, ISIS (depleted) and IPNS (both depleted, D, and enriched, E). However, the problems associated with radiation damage have led to limited operational lifetimes [3] as shown in the table below. Metallic uranium is not suitable for high power sources.

Target	Lifetime MWdays	Target	Lifetime MWdays
ISIS.1	3.08	ISIS.6	4.20
ISIS.2	1.77	ISIS.7	3.57
ISIS.3	5.83	ISIS.9	3.77
ISIS.4	4.63	IPNS.D1	4.5
ISIS.5	9.85	IPNS.E1	2.52

Use of uranium nitride has been proposed for enriched targets [4]. There is, however, very little known about the behaviour of this material in high intensity proton beams. Also there are quite severe problems to overcome to get approval to use targets containing many critical masses of fissionable materials.

4 TARGET COOLING

The distribution of power deposited along a lead target for a 10 cm diameter beam is shown in figure 2.

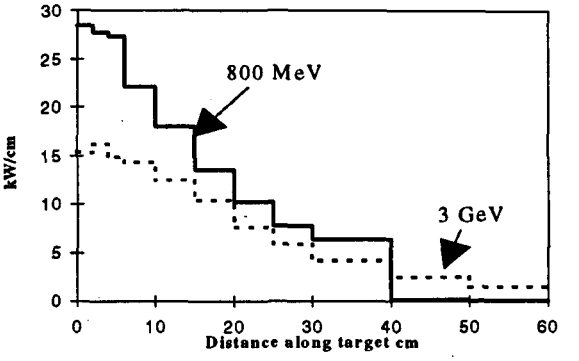

Figure 2. The power deposited along a lead target.

The limit to heat removal is the peak power density in the target and the maximum which can be handled in practical systems is about 4 MW/litre.

The majority of the heat is deposited by the incident proton beam and so for a given beam power the heat distribution in the target can be adjusted by changing the beam energy or current density. Figure 3 shows the peak power density in a Tungsten target as a function of proton energy [5] for a 7 cm diameter beam.

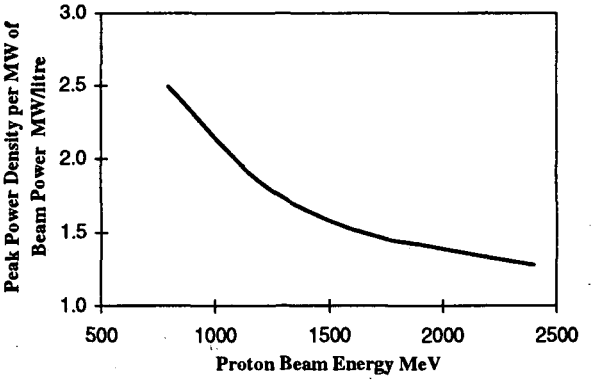

Figure 3. The variation of peak power density with proton beam energy.

Changing the current density can be accomplished by changing the beam size or profile. Figure 4 shows the variation of peak power density in a lead target for a variety of beam profiles and cross sections for a proton energy of 1334 MeV.

The quantity which gives a reliable measure of the heating problem is the current density in the beam. Above about 80 μAcm^{-2} the heat removal becomes problematic.

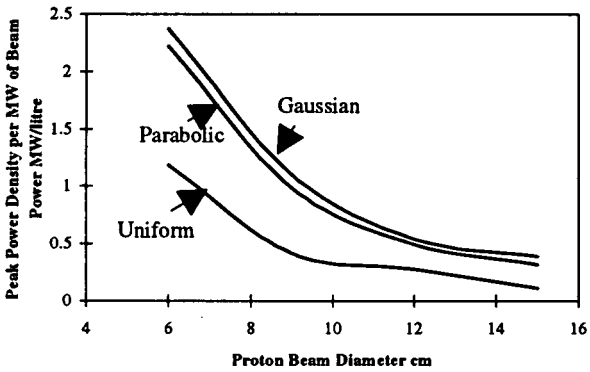

Figure 4. The variation of peak power deposited with beam profile and cross section.

Reducing the power density in the target by changing the beam characteristics will result in a larger target which in some applications is undesirable. There is a limit to the size of proton beams which can be considered practical as well as engineering constraints on the target size.

5 RADIATION DAMAGE

The damage to the target material and containers is generally manifested by embrittlement and has been reviewed in reference [6]. The consequences are a finite lifetime for the target. While a liquid metal target is a natural way of reducing the impact on the target itself, the damage to the target container still remains. As with heat removal, it is the density of interactions which is the crucial factor in determining the effects of radiation damage, so the effects can be reduced, for a given beam power, by increasing the proton beam size or energy. Again the proton current density is a very useful measure of the scale of the effects.

There is limited data available for irradiation effects on materials in a high intensity proton beam. The radiation field in a spallation target leads to much higher production of hydrogen and helium than typical of a reactor. This, and high transmutation rates, makes extrapolation from reactor data very uncertain.

An extensive experiment to measure radiation damage effects in most materials of interest to spallation sources will take place at LAMPF, starting this yea, as part of the Accelerator Production of Tritium (APT) project at Los Alamos [10].

The first ISIS target, irradiated for 60 MWdays, will be dismantled for detailed analysis at KFA Jülich this year. The peak temperature of this target doubled during operation due to the effects of irradiation.

There is considerable scope for development of new alloys suitable for spallation targets and this is the most likely area for improvement in performance in the future.

6 CONTINUOUS AND PULSED SOURCES

6.1 Fast pulse sources

A particular problem exists for targets on pulsed sources. When the duration of the pulse is short the heat is deposited faster than it can be conducted away. The resulting fast temperature rise in a solid target produces high transient thermal stress waves (sometime known as thermal shock). Typically, this will be an important consideration for pulse lengths less than a few microseconds. This effect is also a problem in liquid metal targets where the liquid transmits pressure waves to the target container resulting in high stresses. This is a major concern for the ESS mercury target [7]. Transient thermal stresses may well be the ultimate limit for the power of fast pulsed sources.

A fast pulsed spallation source to provide thermal neutron beams for condensed matter research uses small, typically 0.5 - 1 litre hydrogenous moderators to slow down the fast neutrons from the target. They are sized to maintain short pulses (10 - 150 μs fwhm) and the designs incorporate neutron absorbers to eliminate neutrons moderated by coolant and the reflectors. In this case thermal neutron absorption in the target material is a positive advantage. These systems also require the target to be as compact as possible to maintain high neutron fluxes feeding the small moderators. Increasing the target size leads to a reduction on the neutron beam fluxes.

6.2 Continuous and quasi-continuous source.

For continuous and quasi-continuous spallation sources (pulse lengths ~200 μs or greater) the heat loading does not lead to the potentially high transient thermal stresses of the fast pulse targets. The total number of neutrons produced becomes a crucial quantity and minimum neutron absorption is then vital. This can be achieved by optimisation of the geometry and choice of target material.

For these sources a more extended target generally has less of a penalty in neutron flux than in the case of fast pulsed sources. The consideration of neutron economy is very similar to that in reactor design.

7 SOLID WATER COOLED TARGETS

7.1 Solid targets

All currently operating spallation sources use solid water cooled targets. The TRIUMF facility has a water cooled lead target/beam stop in which the lead melts in the beam region. Low power targets such as KENS and MLNSC at Los Alamos use solid blocks with edge cooling. This technique can be extended to a beam power of about 300 kW as in the AUSTRON study [8]

but is inadequate for much higher power beams. Several designs have been developed which segment the target material into plates, rods or spheres. Examples are described below.

7.2 Plate targets

A schematic diagram of the ISIS target is shown in figure 5. This is typical of plate targets. A stack of plates containing a disc of target material (either tantalum or depleted uranium) is cooled by pressurised water flowing in the 1.75 mm wide gaps between them. The complicated flow arrangement of this target has been designed specifically to give sufficient sensitivity that flow and pressure drop monitoring can detect small <0.2mm) reduction in the cooling gaps as the target material swells. Also this target has an independent water circuit which cools the edges of the plates. This has sufficient capacity to remove the heat from radioactive decay after proton beam turn off

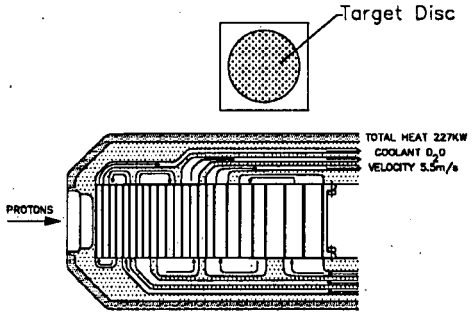

Figure 5. A schematic view of the ISIS target.

A design for a tantalum plate target has been developed for the 5 MW beam of the European Spallation Source study. The principal difference between this and the ISIS target is the thickness of the plates.

7.3 Rod targets

Rod bundles have been used in many reactor designs and this concept has been adopted for the initial target at the SINQ [9] source at PSI.

This is a continuous source and so a low neutron absorption cross section in the target is crucial. The target material chosen is Zircaloy where the low absorption more than compensates for its relatively low atomic mass compared to tantalum or tungsten both of which have substantial absorption cross sections. The target will be developed to use rods made from aluminium tubes filled with lead. Finally a liquid lead, or lead/bismuth target will be used.

Rods are also proposed for the target design of the APT project at Los Alamos [10]. This envisages a 150 MW proton beam at 1.3 GeV which gives 95 MW of heat in the target. To give acceptable power density in the target the proton beam cross section will be 160 cm high by 16 cm wide. This is equivalent to a proton current density of 45 μAcm^{-2} which is about the same as the current density in the existing LAMPF beam stop. So despite the enormous beam power proposed the target does not demand new technology.

The target will be constructed from bundles of tungsten rods about 3 mm in diameter 22 cm long, each tube containing typically 100 rods. Tubes are stacked to give target layers 180 cm high, 25 cm wide and 4 cm thick with a gap between layers. Neutrons produced in the tungsten then escape via these gaps. This design reduces the path length of neutrons in the target material which compensates for the relatively high neutron absorption in tungsten.

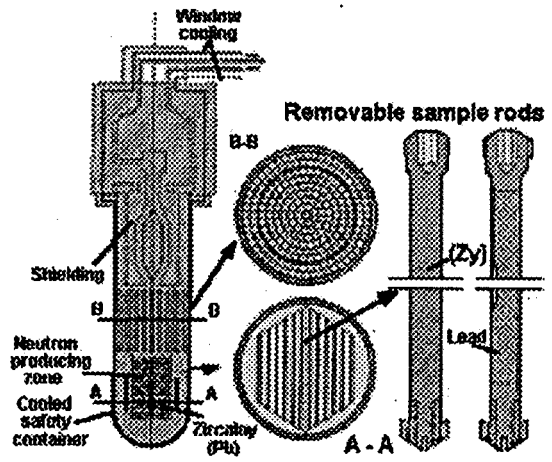

Figure 6. The SINQ target concepts

An alternative to be used for the MLNSC upgrade target and the proposed LPSS [11] source is to have tungsten rods enclosed in helium filled Inconel 718 tubes. The design only relies on radial conduction and so is tolerant of brittle fracture of the tungsten.

7.4 Rotating targets

An alternative way of reducing the power density in the target is to use a rotating wheel. The wheel diameter is typically 1 - 2 m with the proton beam incident on the rim. The speed of rotation is chosen such that an element of the target is fully cooled during one revolution. This concept was studied extensively in the SNQ project [12] and while it has the potential for very high beam powers the target systems are mechanically very complex. The engineering of the rotating seals for the services and the design of the remote handling required are both demanding engineering challenges.

8 LIQUID METAL TARGETS

Liquid metal targets have several advantages. The mean density of the target is not diluted by coolant. They

do not suffer from radiation damage so should last the lifetime of a facility, thus easing the waste disposal problem. There is extensive experience with liquid metal circuits in the reactor industry.

However their use in spallation sources is not without difficulty. Containment in the event of pressure vessel failure is more difficult than for a solid. Lead and lead/bismuth both increase in volume on solidification so a heating system to keep them liquid is essential. Corrosion of the container can take place.

Uncertainty in the effects of radiation damage and transient thermal stress on solid targets has resulted in a mercury target being chosen for both the ESS and Oak Ridge spallation source [13] studies. Mercury has the advantage that no heating system is required to keep it liquid and the thermal neutron absorption is an advantage. The ESS design is illustrated in figure 7.

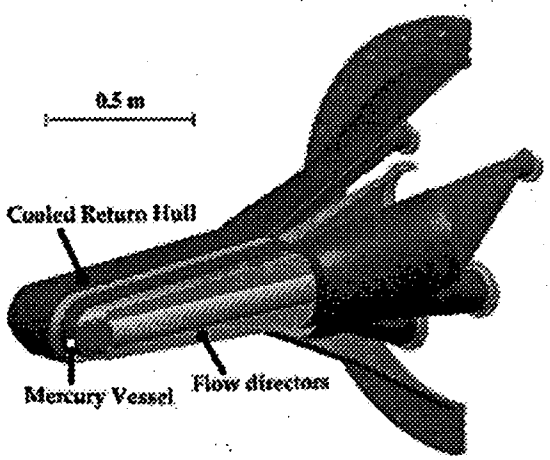

Figure 7. The ESS mercury target.

The ESS is a fast pulsed source with a 5 MW 1.334 GeV proton beam. Early analysis indicates that the pressure waves from the proton pulses result in unacceptable stresses on the container. The current design envisages a system to introduce small bubbles of helium into the mercury to provide compressibility to the target medium and so damp the pressure waves.

This is an illustration that when designed in detail the liquid metal target systems are generally more complex than those of a solid water cooled target. This has to be judged against potentially more reliable operation and in many cases higher neutron fluxes.

7 FUTURE PROSPECTS

The success of the operational sources has shown that high power spallation sources, ~1 MW or greater, have the potential to replace reactors in many applications.

Sufficient success has been achieved in the design studies to give confidence that practical solutions exist for the technical problems associated with the design of target systems. The debate between the relative merits of the basic concepts - solid water cooled, both stationary and rotating, and liquid metal targets, will continue. Novel designs will undoubtedly be developed.

The key question is the behaviour of materials under intense proton bombardment. The fusion programme has had marked success in developing new alloys and there is a clear need for a similar effort to underpin the design of high power spallation targets.

There is every reason to be optimistic about the future. The SINQ source will operate in the near future and there is a good prospect of approval being given for construction of new facilities in the USA. It is to be hoped that these will provide the operating experience which is crucial for the design of future high power spallation targets.

REFERENCES

[1] RSIC Computer code collection CCC-178

[2] J.M. Carpenter, 'Pulsed Spallation Sources for Slow Neutron Scattering' NIM 145 (1977) 91

[3] T.A. Broome, 'Prospects for Targets and Methane Moderators at ISIS' Proc. ICANS XIII, Villigen, 1995 PSI Proceedings 95-02 p.633

[4] Y.Y. Stavissky, 'Spallation Sources at the INR RAS: Present Status and Prospects' Proc. ICANS XIII, Villigen, 1995 PSI Proceedings 95-02 p.63

[5] 'Los Alamos Next Generation Spallation Source' Vol. 1, p.3-24, Report LA-UR-4300

[6] H. Ullmaier, F. Carsughi, 'Radiation Damage Problems in High Power Spallation Neutron Sources', NIM B 101 (1995) p.406-421

[7] G.S. Bauer, 'A Liquid Mercury Target for the ESS' Contributions to the fourth general ESS meeting', Weinfelden, (1995), ESS report 95-34-M

[8] H. Schönberger, 'AUSTRON - A Spallation Neutron Source for Central and Eastern Europe' Proc. ICANS-XII, Abingdon, 1993 RAL report 94-025 p.P-26

[9] G.S. Bauer, 'SINQ-Status Report Oct. 1990' Proc. ICANS-XI, Tsukuba, 1990 KEK report 90-25 (1991) p.41-60

[10] 'Design of the APT Target/Blanket Design, Revision 2.0', LANL report LA-UR-95-3233

[11] 'Los Alamos Next Generation Spallation Source' Vol. 2, p.2-13, Report LA-UR-4300

[12] G.S. Bauer, 'The General Concept for a Spallation Neutron Source in the Federal Republic of Germany', Atomkernenergie-Kerntechnik 41 (1982) p.234-242

[13] B. Appleton, 'Status of the Oak Ridge Spallation Neutron Source (ORSNS) Project' Proc. ICANS XIII, Villigen, 1995 PSI Proceedings 95-02 p.814

BEAM INDUCED RADIATION PROBLEMS AND CURES

P. E. Gear
Rutherford Appleton Laboratory
Chilton, Didcot, Oxon. UK.

ABSTRACT

ISIS, the high intensity pulsed neutron source at the Rutherford Appleton Laboratory, operates with a mean proton beam power in excess of 160 kW at a beam energy of 800 MeV. Beam loss is controlled to prevent damage to machine components and localise high levels of induced radioactivity. A description is given of how ISIS is operated so as to minimise the induced activity. Details are provided of the procedures and formalised methods of control that enable the manual handling of activated machine components within limited, collective personnel doses.

1 INTRODUCTION

ISIS, the high intensity accelerator based pulsed neutron source at the Rutherford Appleton Laboratory (RAL), now operates regularly at its design intensity of 200 μA (2.5 E13 ppp at 50 Hz). This is equivalent to a mean proton beam power of 160 kW at the extracted beam energy of 800 MeV. Operating with such beam power could, due to uncontrolled beam loss, result in severe component damage and give high levels of induced radioactivity. Such damage is invariably unexpected, disruptive to scheduled running and expensive in several ways. There will be increased costs, involving financial and personnel resources, in providing for the manufacture and rebuild of spare components, the provision of secure active waste storage areas and the eventual disposal of the damaged but highly active component. The requirement to provide additional compensating operating time may effect other planned work. There will also be the possible loss of goodwill from the scientific community.

Somewhat lower levels of beam loss may give less component damage but could give, over a period of time, such high levels of induced activity that a manual 'hands-on' or 'active handling' maintenance regime, such as that used on ISIS, would not be possible. (Remote handling techniques are necessary in the target station and will not be discussed here).

It is therefore necessary at all times to operate in a manner which minimises beam loss (and therefore induced activity levels) and to have in place methods of working which ensure that the requirements of the UK Ionising Radiation Regulations 1985, which are based upon the International Commission on Radiological Protection recommendations, are met.

2 GENERAL CONSIDERATIONS

Induced activity is a major hazard on ISIS (contamination much less so). The Ionising Radiation Regulations calls for the setting up of radiation controlled areas, the issuing of Local Rules and the appointment of Radiation Protection Supervisors and a Radiation Protection Advisor, who ensure compliance. It also gives three principles for work in active areas:

- every practice resulting in an exposure to ionising radiation shall be justified by the advantages it produces;
- all exposures shall be kept as low as reasonably achievable (ALARA);
- that specified dose limits shall not be exceeded.

In order to comply with the first principle each and every entry to a controlled area must be justified on the basis that it is necessary in order to maintain the facilities operational status. To maintain a 'hands-on' maintenance regime, and to comply with the second and third principles, ISIS is operated so as to minimise beam loss. Experienced operators continuously observe

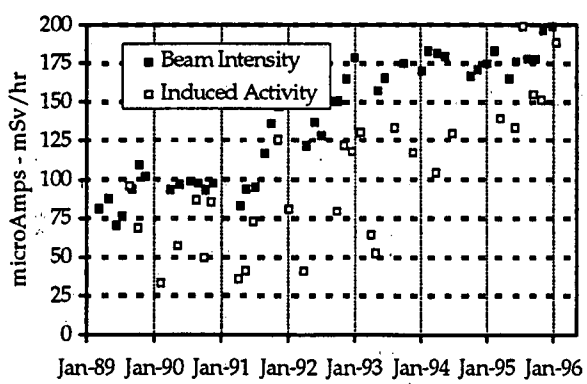

Figure 1. Average beam intensity/induced activity.

machine conditions and monitoring systems are used to detect beam loss and trip off the beam if such loss exceeds predetermined levels. There is, however, always beam loss, caused during machine setting up and machine physics periods and by the inefficiencies of the beam trapping or acceleration processes, beam instabilities, beam/residual gas scattering, failure of components or incorrect operation of the accelerators. This beam loss will result in above background levels of induced activity of components. Fig. 1 shows a correlation between average 'beam on target' operating intensity and total induced activity. This has occurred

even though the allowed rate of beam loss has been maintained constant over the period.

3 MINIMISING BEAMLOSS

3.1 General operational control

Minimising beam loss, at all operating levels, is achieved in the first instance via administrative action by the operation crews, headed by an experienced Duty Officer. Following laid down and frequently reviewed operational procedures, changes in machine characteristics and performance are acted upon immediately. Continuous on-line information e.g. beam loss spill, beam intensity and position and various efficiency factors, provides the Duty Officer with sufficient data for him to be able to assess and judge the performance of the accelerators and to take any action as necessary. An 'on call' system enables advice and support to be available 24 hours a day during operational periods. Backing this operator (or manual) system of control are two independent monitoring systems operable at all machine repetition rates except 'base rate'. Used when beam physics experiments, setting up operations or when investigation of fault conditions is required, this default repetition rate (50/32 Hz) enables such work to proceed unhindered by frequent interruption to beam. Such periods of operation, which can lead to an increase in activity levels, are carefully controlled.

3.2 Beam loss monitoring system.

Previously described [1], the beam loss monitoring system (BLM's) provides a real time on-line display of prompt beam loss, together with beam warning, automatic beam trip and data logging. Analogue signals from each of 66 ionisation chambers, located close to the accelerators and extracted proton beamline, are integrated over the appropriate machine pulse lengths and fed to three dedicated graphics displays in the Main Control Room (MCR). These beam loss displays, covering the linac, synchrotron and extracted proton beamline, are a powerful diagnostic during machine running providing 'at a glance' indication of correct machine running. The integrated signals are also fed to a beam interlock unit where any signal greater than a predetermined level will result in either a warning or the beam being tripped. This monitoring, carried out on a pulse by pulse basis, gives a warning message for one pulse above the trip level and initiates a beam trip for 20 consecutive pulses above the trip level i.e. within 400 msec. Each analogue signal can also be accessed and monitored for diagnostic purposes.

The distribution of prompt beam loss, as shown by the synchrotron BLM's, and taken with ISIS operating at a beam current of 200 μA (2.5 E13 protons per pulse), is shown in Fig. 2. As can be seen the loss is confined to superperiods 1 and 2 where graphite beam collectors

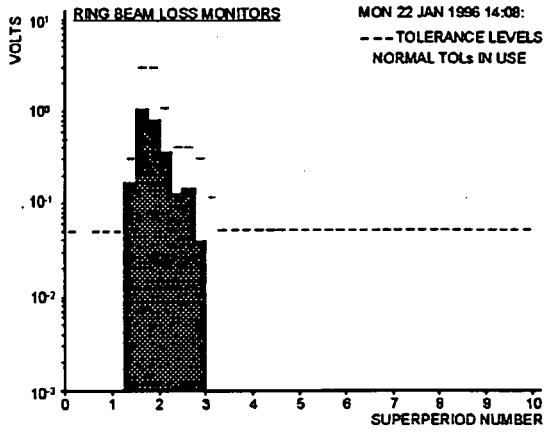

Figure 2. Prompt beam loss in the synchrotron.

intercept beam lost in the trapping process, typically of the order of 12%. There is no loss in the rest of the ring above the 1 mV level. The horizontal bars indicate the trip level allocated for each loss monitor. A typical trip level outside superperiods 1 and 2 is 50 mV, equivalent to a beam loss of 1 E11 ppp at injection and 2 E9 ppp at extraction.

3.3 Beam Intensity monitoring system.

The intensity monitoring system, based upon the analogue signals derived from toroidal current transformers, provides real time intensity data from the accelerators and the extracted proton beam line. In a system analogous to that for the BLM's described above, the signals are processed to give efficiency figures, data logging and a beam loss warning and beam trip facility.

The individual analogue signals are also available for diagnostic purposes. Displays in the MCR give the intensity in protons per pulse, and efficiency figures, derived from the intensity data, for the injection, trapping, acceleration, extraction and extracted beam transport processes. Warning of increased loss of intensity for any of the above processes is given over two time periods, 20 minutes and 30 seconds. Automatic beam trips are initiated either for a 25 pulse averaging loss, or for 3 consecutive pulse loss. The beam is therefore switched off in 60 msec, before any severe damage might occur.

The current intensity loss warning and trip levels are shown in Table 1. With these levels and an injected beam of 2.9 E13 ppp, warnings of increased injection loss are displayed for loss exceeding 3.1%, averaged over 20 minutes, and for loss exceeding 4.5% averaged over 30 seconds. A beam trip will occur for loss

Table 1. Tolerances for Intensity Loss (1988 levels in brackets).

LOSS AT (protons/pulse)	20 MINUTES WARNING	30 SECONDS WARNING	25 PULSE AVERAGING TRIP	3 PULSE IMMEDIATE TRIP
INJECTION	9.0 E+11 (7.0 E+11)	1.3 E+12 (1.0 E+12)	1.5 E+12	4.9 E+12
TRAPPING	4.2 E+12 (1.5 E+12)	4.3 E+12 (2.0 E+12)	4.5 E+12 (3.0 E+12)	4.9 E+12
ACCELERATION	2.0 E+11 (7.0 E+11)	2.5 E+11 (1.0 E+12)	5.0 E+11 (1.2 E+12)	2.0 E+12
EXTRACTION	1.0 E+11 (2.5 E+11)	2.0 E+11 (4.0 E+11)	5.0 E+11	1.0 E+12
EPB LINE	6.2 E+11 (1.5 E+11)	6.5 E+11 (3.0 E+11)	7.0 E+11 (5.0 E+11)	1.0 E+12
TOTAL LOSS	5.2 E+12 (2.0 E+12)	5.6 E+12 (2.5 E+12)	6.0 E+12 (3.0 E+12)	6.1 E+12 (4.9 E+12)

exceeding 5.2% averaged over 25 pulses and for loss exceeding 16.9% for three consecutive pulses. These tolerance levels are quite tight when compared with the typical 2-3% loss currently achieved.

The two independent systems provide different but complementary levels of protection. The beam intensity monitoring system gives early warning of increased beam loss and a fast beam trip in the event of equipment malfunction, whilst the more sensitive BLM system can detect and act on loss, caused for example by equipment instability, not detected by the beam intensity system.

4 INDUCED ACTIVITY

Over 200 hundred predetermined points around the accelerators are regularly monitored for levels of induced activity, usually prior to any maintenance or installation work. This data is analysed, in a spreadsheet format, to give information regarding trends in induced activity and therefore changes in accelerator operating conditions. The histogram, Fig 3, shows the average 'on contact' induced activity for all superperiods of the synchrotron, except superperiod 1 (SP1), together with the injection (HEDS) and extraction beam transport lines (EPB). The beam collectors situated in SP1 give high levels of activity > 50 mSv/hr, and are only measured when necessary.

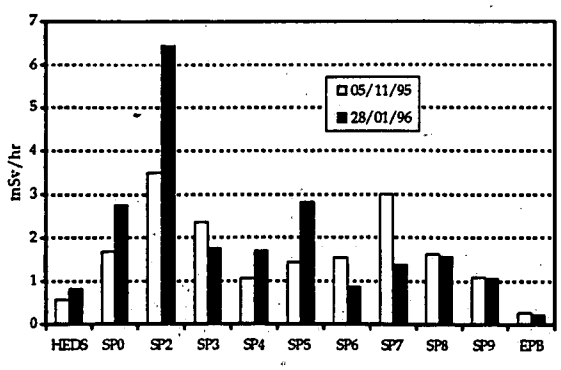

Figure 3. Average induced activity.

The two sets of data shown cover the period of the recently achieved 200 μA operation and show that the induced activity has increased in the HEDS, in SP0, (the injection area) and in SP2, 4 and 5. In the other areas of the synchrotron the induced activity has actually decreased. It is possible to continue this type of analysis by looking at the loss patterns making up, for example, the increased loss in SP2 so giving trends of loss on particular components. Correlation is then sought with accelerator operating conditions.

This data, whilst useful to the machine physicists, is of primary importance when planning and scheduling maintenance and installation work. It is clear, from Fig. 3, that even in the 'cooler' areas of the accelerator, on contact levels are at or approaching the 1 mSv/hr level. Personnel working in these areas could therefore receive high radiation doses in a very short time. Forward planning and control of all work is therefore essential if dose levels are to be minimised. The data is also available to project engineers responsible for the design and modification of components enabling them to be kept up to date and aware of the level of hazard that may be met in any particular area of the machine.

5 WORK IN RADIATION CONTROLLED AREAS

It was recognised in the early stages of ISIS that good design practices and the use, where possible, of time saving devices built into components would reduce installation and removal times. These devices range from the use of kinematic mounts, so that components can be pre-aligned before installation, to the use of 'quick

disconnects' for electrical and water connections. A manual hands-on maintenance regime could not be sustained without such devices and their continual design and development.

Planning is an essential part of dose minimisation and a written hazard assessment, for each major job, is prepared by the project engineer together with the installation engineer and Health Physics advisors. This assessment breaks down the job into its component tasks and, after determining induced activity levels around the area of work, allocates a time to each task and the expected dose to personnel. Extensive use is made of photographs, drawings and previous experience. Any requirement to design, manufacture and test special shielding or tools will be highlighted. Detailing the work in this way enables possible problems to be discussed, identified and resolved before the work starts. Trial or dummy runs are performed for major new installations and these will often highlight potential installation problems.

The nature of work carried out in the radiation controlled areas range from relatively simple and quick maintenance jobs, such as replacing failed vacuum gauge heads, to complex jobs such as replacing a magnet assembly which can involve many different and often complex tasks. It is important that a high degree of control is exerted for all work, however simple, and at all stages, so as to minimise occupancy of the radiation controlled areas.

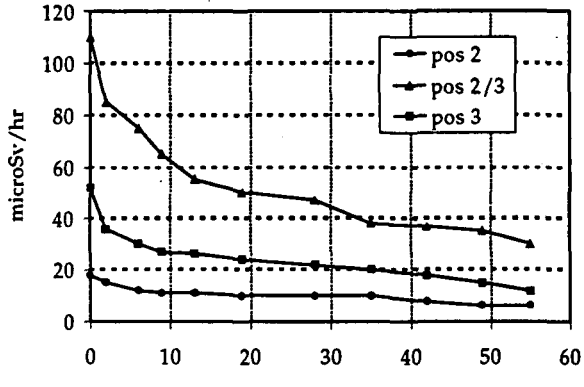

Figure 4. Synchrotron induced radiation decay.

All work in the controlled areas must be authorised by the Duty Officer who, in his capacity as a Radiation Protection Supervisor, is responsible for ensuring that all work in radiation areas satisfy the requirements of the Ionising Radiation Regulations. He carries out a detailed induced activation survey of the work area and assesses each separate job to be undertaken. He will be advised by health physics personnel especially when a job hazard assessment has been prepared. If necessary he issues a Radiation Permit to Work to the work supervisor, which details, amongst other things, dose limit, personal dosimetry to be worn and the precautions and conditions that need to be taken in order to minimise the overall dose. This Permit is signed by all personnel engaged in the activity signifying that they understand the nature of the hazard and the conditions and precautions that apply. All work, once underway, is continually assessed by the Duty Officer and Health physics personnel to ensure that conditions of the Permit are being followed and that dose levels are not exceeding expected levels. In addition, the project and installation engineers will continuously monitor work progress with reference to the hazard assessment and the received dose.

Minimising collective dose for all work in active areas involves the use of one or more of the following standard methods for radiological protection against external radiation - Time - Distance - Shielding.

5.1 Time

The collective effect of the natural half-life decay of the various nuclides making up the overall induced activity level is shown in Fig. 4. During the first 8 weeks of a major shutdown there is an initial steep decay, over the first 10 to 15 days, followed by a more constant decay. To obtain the maximum benefit from this natural decay no major installation or maintenance work, in the more active areas, is scheduled to start earlier than 20 days into a shutdown. Restricting time of occupancy in active areas, as detailed in the hazard assessment, is another important feature in minimising dose.

5.2 Distance

In a hands-on regime it is almost always beneficial to operate at a distance with, for example, long handled devices.This is not true if an increase in operating time

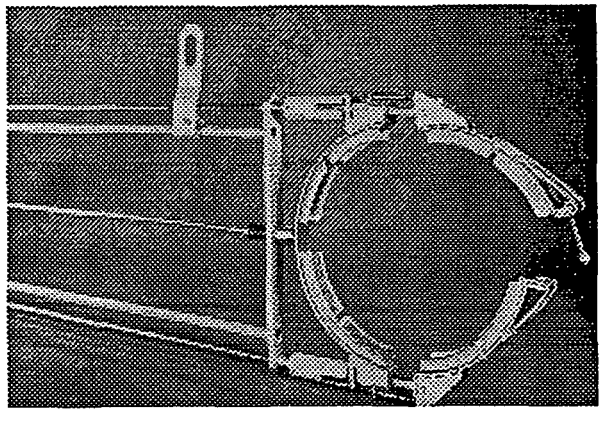

Figure 5. Long-handled vacuum clamp.

in using a device counteracts the benefit of distance. They must, therefore, be well designed for quick and simple operation. They are especially effective for

repetitive tasks where many similar tasks are required to be carried out. An example is the device for making and breaking UHV vacuum clamps in the synchrotron, Fig. 5. This enables an operator to remain at a distance of over 2 metres so reducing the operator-received dose by over an order of magnitude.

5.3 Shielding

Use is made of a variety of shielding techniques to reduce background activity to levels were work is assessed as able to proceed. Large concrete blocks are manipulated into position to shield open areas from gross radiation effects. These cannot however, due to their bulk, easily provide localised shielding around equipment and beam pipes and so use is made of purpose built contour or profile shielding, Fig. 6, and local personnel shields to give more detailed protection. Constructed of lead, and lead glass for windows, they can easily be craned into position from a distance. Lead sheet is extensively used to provide additional local shielding as required.

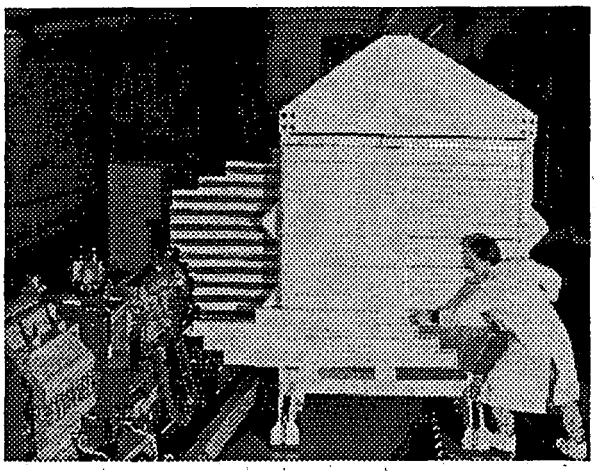

Figure 6. Profile Shielding

It is clearly of benefit to use, whenever possible, a combination of the above three methods of radiological protection and install purpose designed equipment, especially where frequent and immediate access to active areas is necessary. An example is the new semi-automated foil change mechanism, which has a lengthened loading platform, automated vacuum and foil loading processes, and purpose built shielding. These changes, when compared with the previous foil change mechanism, have increased the distance from active components, reduced the time of occupancy and reduced the ambient induced activity levels. The overall effect has been to reduce the collective dose for a foil change by a factor of five. The creation of a less stressful environment is an added benefit. and has resulted in foil replacement, which requires a calm approach and a steady pair of hands, being carried out more successfully.

6 CONCLUSIONS

ISIS operates a hands-on regime for all work in the accelerator areas. Control of beam loss by means of administrative action and by automatic beam loss warning and beam trip systems minimises beam loss during operational periods. Suitable design of components facilitate the easy removal and adjustment of equipment. Procedures and methods of assessment are used to control rigorously all work carried out. That these controls and procedures are increasingly successful can be seen in Fig. 7. A generally falling level of collective dose, for all ISIS personnel, has been achieved in spite of increased operating intensity and induced activity levels. No individual has received a dose of more than 5 mSv in any year.

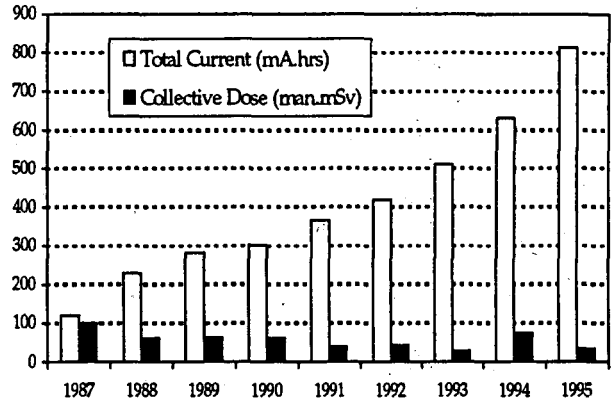

Figure 7. Collective dose rates.

These collective dose levels are also consistent with operating an 'active handling' maintenance regime within the reduced occupational dose limits currently being promulgated.

7 ACKNOWLEDGEMENTS

The continuing successful operation of the ISIS accelerators is due to the dedication and resourcefulness of all staff in ISIS Source Divisions.

8 REFERENCES

[1] M.A. Clarke-Gayther, A.I. Borden and G.M Allen, Global Beam Loss Monitoring Using Long Ionisation Chambers at ISIS. Proc. EPAC 94, London, 1994, p 1634.

The Use of ISIS as a Proton Therapy Facility

D.J.Adams, C.M.Warsop, M.R.Harold, I.S.K.Gardner, ISIS Facility, RAL, Oxford, UK.

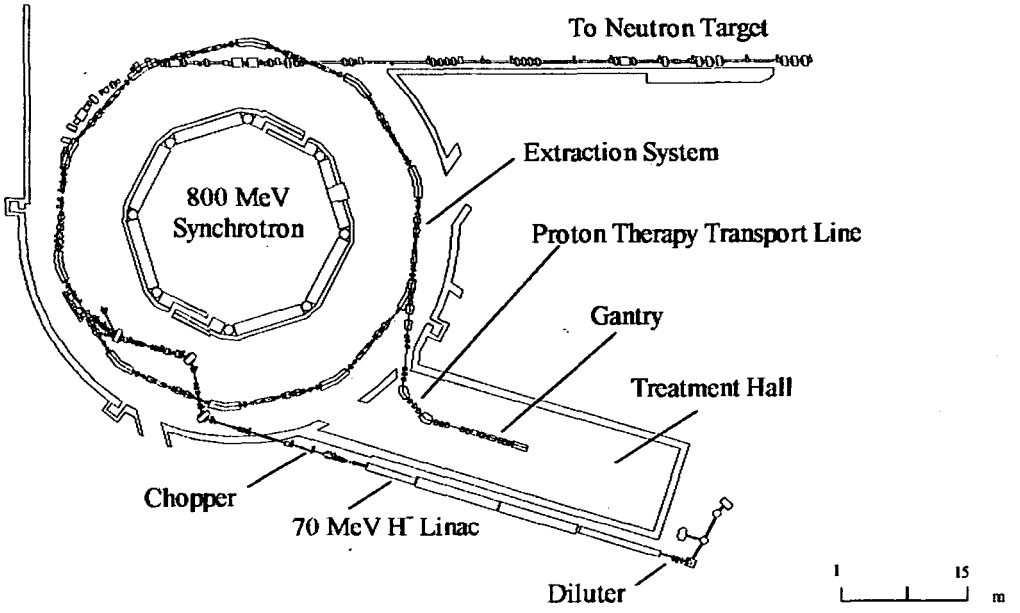

Fig 1: Layout of the ISIS facility with the proposed modifications for the proton therapy facility.

1 Introduction.

ISIS is the Spallation Neutron Source at the Rutherford Appleton Laboratory in the UK, designed and built for condensed matter research. Following recent studies reviewing possible medical applications of the ISIS Accelerators [1], the UK Medical Community has shown considerable interest in development of a Proton Therapy Facility. A collaboration, 'PROTOX', which includes the Oxford Radcliffe Hospital and RAL, is now engaged in preliminary studies, investigating how such a therapy facility might be realised.

Clearly, such a project will have to represent a significant cost saving compared with a new, purpose built facility. It is hoped a UK facility, comparable with those at PSI in Switzerland [3,4] and Groningen in Holland will be possible. The medical remit of the project would include clinical trials and substantial research: it would form the pilot project for developing proton therapy in the UK. In this paper, an outline is given of how a workable proton therapy centre might be incorporated in the ISIS Facility.

2 Medical Requirements.

Specific aims of the project are to provide conformal therapy using the spot scanning technique, and multiple treatment directions with an isocentric gantry.

Spot scanning builds up a conformal dose by dividing the tumour volume into many elements, and dosing each element sequentially. This requires a well controlled, stable beam, with widths and positions defined to 1 mm and typical energy spreads of 0.1%.

Proton therapy also requires beam energies in the range 70-225 MeV, accurate to 0.1%, to treat tumours at all depths. Beam intensities of approximately 2×10^{10} protons per second are needed (5 Gray/min), to keep treatment times to a few minutes. Intensities should be controllable over a wide dynamic range to an accuracy of 1%.

3 Proton Therapy Facility.

3.1 Review of the ISIS Facility

The facility consists of a 70 MeV H^- injector, an 800 MeV fast cycling proton synchrotron, beam transport lines and a spallation neutron target (see Figure 1). During the multi-turn charge-exchange injection process, 2.8×10^{13} protons per pulse are accumulated over 200 μs from the 20 mA injector beam. After injection, protons are accelerated to 800 MeV in 10 ms, then extracted in a single turn and transported to the heavy metal target. The machine repetition rate is 50 Hz, and pulse lengths in the synchrotron are of the order of 1 μs.

3.2 Proposed Scheme of Operation

The proposed scheme utilises the present linac and synchrotron, with modifications, and makes use of an existing building. The principal new systems required are: an intensity reduction system, specialised diagnostics, a new fast extraction system, a beam transport line and a gantry.

The 10^{10} protons per second required for proton therapy correspond to intensities of $2x10^8$ protons per *pulse* at the ISIS repetition rate of 50 Hz - thus intensities must be reduced by a factor of 10^5. A two stage intensity reduction system is envisaged, using a beam diluter and fast chopper prior to injection. Once the correct intensity has been injected into the synchrotron, the beam is accelerated and the desired beam energy selected by extracting at the appropriate time. The new fast extraction system would deflect the beam vertically into a purpose built beam line, which transports and matches the beam to the therapy gantry. The spot scanning system, incorporated in the gantry, would then direct the beam appropriately. Up to 10^4, 1 μs beam pulses (spots) at 50 Hz would be available per treatment session.

It is an essential prerequisite that proton therapy running would not interfere significantly with neutron production. To this end it is proposed that the accelerators be dedicated to therapy for 5 minutes per hour, the remaining time being required for neutron production. An option to run at 0.8 Hz during normal neutron production, for set-up and diagnostics, is also a possibility.

In the following sections the key features of the project are outlined, indicating areas where further work is required.

4 Beam Control and Stability

The high intensity accelerators of ISIS were not designed with the stringent requirements of proton therapy in mind, therefore research will be required to ensure appropriate levels of control and stability are achieved. In particular, the time structure of ISIS is very different from existing facilities, and introduces some significant problems in dose control and verification. Initial plans for beam control systems are given below.

4.1 Intensity Control.

To reduce the normal ISIS beam intensity from 10^{13} to 10^8 protons per pulse, two measures are proposed. First, a reduction in the injector current by a factor of 1000 using a beam diluter, and second, a reduction of the injection pulse length by a factor of 100 using a fast beam chopper, as in Figure 2. Varying the injected pulse length allows fine control of intensity; beam would be injected until the required intensity is measured in the synchrotron. This measured intensity would then be extracted, and delivered to the patient. The precise operating details are presently under study.

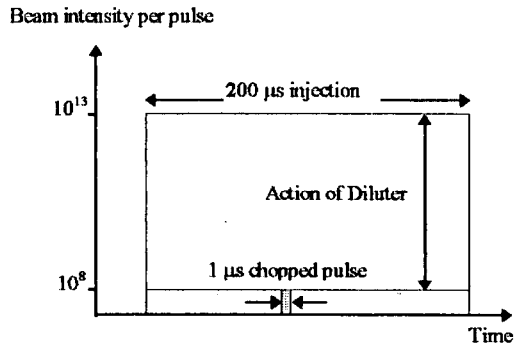

Fig 2: Proposed Scheme for beam reduction

4.2 Transverse Beam Size and Position.

In order to moderate beam line and gantry costs, apertures are to be kept to a minimum. Injector beam emittances are ~25 π mm mr in both planes, and it is expected that the emittance of the extracted therapy beam would be similar. Therapy beam line acceptances of ~40 π mm mr are thus proposed, which are also compatible with use of the PSI Gantry design (see below).

In contrast to injection under high intensity operation, where phase space painting fills much of the (~400 π mm mr) synchrotron acceptances, therapy operation will require minimal increase of emittances during injection. Consequently precise control of injected profiles and positions will be required, and possibly some collimation.

Accuracy and stability of beam position (±1 mm) at the patient demands a well controlled, stable beam at the extraction point in the synchrotron: this will require development work.

4.3 Energy Control.

The beam energy delivered to the medical transport line is controlled by extracting at an appropriate time during the acceleration cycle of the synchrotron. Precise selection of energy (±0.1%) would be achieved by counting beam revolutions; some checks on stability and a method for calibrating absolute energy will be necessary.

4.4 Diagnostics.

In order to achieve the control described above, new diagnostics operating in an intensity regime of 10^8 protons per pulse would be required. Suitable intensity toroids, position monitors and profile monitors for the injector, synchrotron, beam lines and gantry, will need to be developed. Recent studies using chopped beams purely for machine studies [5], at intensities of 10^{10} protons per pulse, have given some relevant experience.

5 Beam Transport Line and Gantry

An existing gantry design in use at PSI [3,4] is in many respects ideal for PROTOX. It incorporates spot scanning, is compact, and has compatible acceptance. The design is based on a 360° isocentric gantry, with an eccentrically mounted patient platform, that allows a small overall radius of 2 m. A spot scanning system is incorporated into the gantry design, which allows active scanning of the beam in the bend plane. Scanning in the remaining transverse plane is achieved by moving the patient on a transporter.

The gantry optics have been designed to deliver a transverse beam shape which is effectively independent of gantry orientation. This is achieved by designing the optics to be symmetric, reproducing the input beam parameters at the gantry isocenter. Thus a circular input beam remains effectively unchanged irrespective of gantry orientation. The gantry is achromatic in the plane of bend to promote beam stability and to simplify transverse coupling effects.

The beam transport line carries the therapy beam from the synchrotron and matches the beam to the gantry. The boundary conditions imposed by the gantry require the transport line to deliver a circular, achromatic beam. The spot scanning system requires a flexible spot diameter and beam profile which minimises dose to skin and intervening healthy tissue. Therefore the transport line should also produce a controllable beam diameter at a waste. The beam optics of this system are under study. An option to incorporate momentum and beam size collimation is also under consideration.

6 Energy Variation

ISIS has the ability to vary the treatment energy on a pulse to pulse basis by timed extraction from the synchrotron.

Controlling the extraction system, transport line, gantry and spot scanning system at 50 Hz (matching the magnet fields to the extraction energy) would allow a clean, well defined treatment pulse to be used. This system represents the most accurate solution in terms of treatment energy and intensity control but would be expensive to build.

Alternatively, the beam could be degraded to the treatment energy from a single or limited number of extraction energies. The disadvantages of degrading are the associated uncertainties in energy, intensity and position, which are undesirable for spot scanning. A 'range shifter' system in use at PSI, comprising 36 plates, can vary the treatment energy by 2-5 MeV per plate, depending on the incident beam energy. A similar arrangement could be used on ISIS, and would simplify matters considerably as the extraction system, beam line and gantry would only need a few fixed momentum settings. The merits of both possibilities are under consideration.

7 Safety

A full safety audit will be needed before design proposals are made. However, the proposed scheme has many implicit safety features. Dedicating the machine to proton therapy for 5 minutes ensures no high intensity pulses are in the machine during proton therapy sessions. The proposed method of intensity control allows for multiple checks on pulse intensity before extraction to the therapy beam line: aborting unsatisfactory pulses is easily achieved by inhibiting extraction.

8 Conclusions

Preliminary studies suggest that a workable, technically feasible and medically useful proton therapy facility on ISIS may be possible. There are a number of key areas in which details need to be established before any proposals are made, and it is hoped funding will be found to allow the necessary study. PROTOX could be an excellent opportunity for development of proton therapy in the UK.

References

[1] Possible medical applications of the ISIS accelerators. D J Adams, C M Warsop and M R Harold, ISIS/SYN/1/95.

[2] Spallation Neutron Source: Description of Accelerator and Target, B Boardman, RAL Report RL-82-006, 1982.

[3] The 200 MeV proton therapy project at the Paul Scherrer Institute: Conceptual Design and Practical Realisation. E Pedroni et al, Medical Physics, vol. 22, No 1, Jan 95

[4] Beam optics design of compact gantry for proton therapy. E Pedroni.

[5] Low Intensity and Injection Studies on the ISIS Synchrotron. C M Warsop, Proceedings of EPAC 94.

REDESIGN OF THE 90° ANALYSING MAGNET OF THE ISIS H⁻ ION SOURCE USING FINITE ELEMENT MODELLING

C.P.Bailey, RAL Didcot UK.

1 ABSTRACT

The magnetic field strength, uniformity, and stray components of the ISIS penning H⁻ ion source 90° bend magnet have been measured and modelled, both showing the intended steering is not achieved. If the field strength and particle energy are set to cause the particles to follow a constant radius, the resulting bend after passing through the fringe fields is 99°. Thus in use the energy and field strength are mismatched, in order to reduce the bend to 90°, which results in the beam following a path of increasing radius. This generates aberrations and causes the beam to be offset.

The design has been altered by shortening the pole pieces, and by adding a tube of high permeability material, to control the fringe fields along the beam path. The models of the new configurations show the beam can, after following a constant radius path through the magnet, be aligned. There is always a small offset but the magnet and source can be repositioned to take account of this. The position of the tube can be adjusted longitudinally which changes the overall bend angle.

2 DESCRIPTION

The ISIS ion source analysing magnet is designed to operate with a field index of n=1. [1,2] However, in order to achieve maximum extracted beam current, it is operated at a field level significantly lower than that required for n=1 operation at the ion source extraction voltage. A finite element model of the magnet, shown in figure 1, has been developed to investigate this effect using the Vector Fields Opera3d software. This model has shown that despite the original pole design being cut off at 80°, the beam is bent through ~99°, when the fields are set for n=1 operation. Thus the shortening is inadequate to control the effects of the fringe fields. The over steering is compensated by the reduced field level operation. The beam does not remain on constant radius as it would under n=1 conditions, but drifts wide, introducing aberrations. While it emerges close to parallel with the axis it is displaced below it, and consequently misaligned with the downstream elements of the beam line, risking further aberrations and steering.

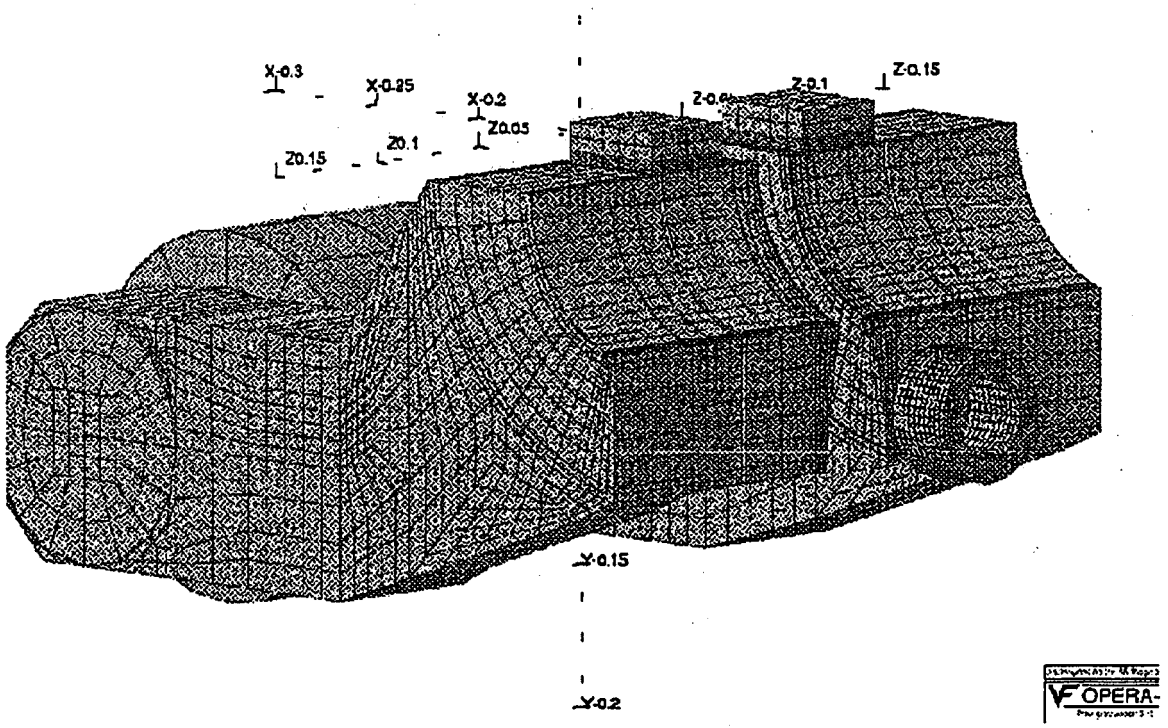

Figure 1 Magnet Model.

There are constraints on any modifications to address this problem. There is a requirement for a residual field, to sweep stripped electrons from the beam before the next components. The total length of the ion source and analysing magnet system is limited by space restrictions in its intended location.

2.1 Probe beam definitions

The steering produced by the magnet was investigated using the particle tracking code built into the software. Initially using single particles and ribbon beams with extent in only one phase plane. These simulations highlighted the steering problems but did not show aberrations. The more promising models were re-examined using a beam defined in both phase planes. This beam takes points around the bounding ellipse in one phase plane and at each of these takes an equal number of points on the bounding ellipse in the other plane. The beam is 20 mm by 20 mrad in the x-plane and 2 mm by 200 mrad in the y-plane. The beam size parameters are calculated by passing the tracking data to a mathcad program that converts from the position and axial velocities produced to conventional xx′ phase space. The accuracy of this process is limited by the need to find a suitable compromise between the number of particles and an acceptable processing time. A maximum of 225 particles has been used. The beam size is calculated by fitting an ellipse around all the tracked particles, after allowing for displacements from the axes.

2.2 Possible modifications investigated

The effects of changing the pole piece design and adding a shielding tube downstream of the poles have been modelled, and the effectiveness of these changes investigated using the particle tracking described earlier. Although it is possible to achieve correct alignment of the central trajectory solely by shortening the pole pieces to between 72° and 73°. This results in the beam traversing an extended region of fringe field, causing beam steering to vary across the magnet aperture.

Options using both shortened pole pieces and a tube, in the space available give too little steering. Unless the tube is so small it has almost no effect or the reduction in pole length is small.

2.3 Comparison of tube only solution with operational design.

The use of a tube, of high permeability material, and the original pole pieces is the most promising. The effects of varying the gap between the magnet and the tube have been modelled. The tube size used is 30 mm inside diameter, 8mm wall thickness and 25 mm long. The wall is sufficiently thick that it does not saturate and small enough that the reduction of the main field strength, within the magnet poles, is easily compensated. A simple tube has been chosen as it shields the beam adequately, eliminating the unwanted steering. The length of 25 mm is a compromise that allows the beam to exit into a region of suitable field for electron sweeping independent of the gap length. Using a constant main field strength the changes in the final alignment caused by varying the gap between the poles and the tube, are shown in table 1.

Table 1 Steering effects of gap length.

gap	resultant angle	displacement
31 mm	-5 mrad	-4 mm
36 mm	-1 mrad	0 mm
41 mm	10 mrad	-2 mm

Subsequent tests concentrated on the 36 mm gap as the improved design. Using the beam with both x and y extent. Figures 2, 3 and 4 show the results for the different models of calculations at the output for; a) The spot size, b) Horizontal emittance, c) Vertical emittance. The ellipse areas for each of these parameters are listed in table 2. The values for the 36 mm gap design, operating at n=1 field for 16 and 18 kV extracted beams, are compared with the operational design with the field level set for n=1 operation, ignoring the steering error, and with the field at the operating level.

Table 2 Beam sizes after magnet.

model	xy mm^2	xx′ mm mrad	yy′ mm mrad	y centre mm	y′ angle mrad
n=1 ignoring mis-steer (i)	174.1	188.9	177.9	1.8	85.1
Operational design (ii)	224.8	209.7	211.4	-10.2	-3.1
36 mm gap full field (iii)	173.7	209.3	181.7	0.0	-0.8
36 mm gap reduced field	177.8	197.8	184.9	-2.0	-1.8

Figure 2 shows the central trajectories for the first three cases listed in table 2. The steering correction in the improved design also causes the y-plane emittance to be closer to the level of the operational design at the unusable n=1 field level. The emittance in the x-plane seems to be related to the field level in the magnet rather than the path taken by the beam.

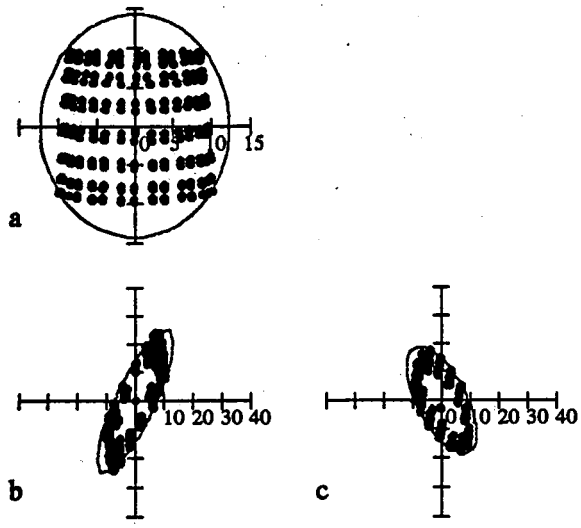

Figure 2 original specification

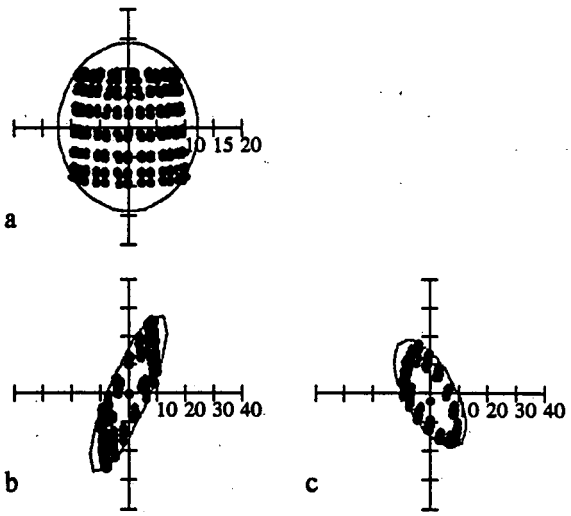

Figure 4 36 mm gap full field

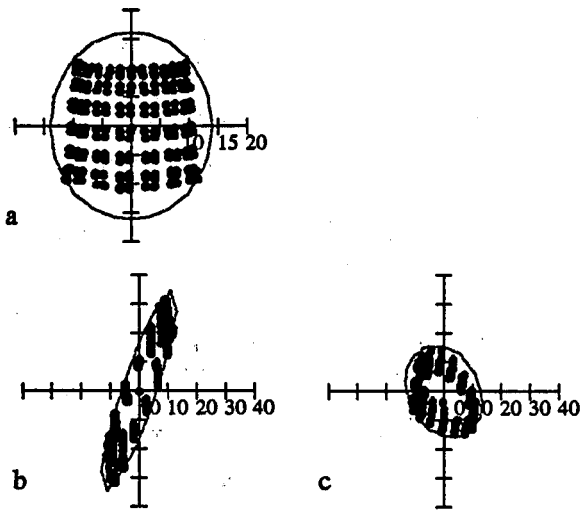

Figure 3 operating conditions.

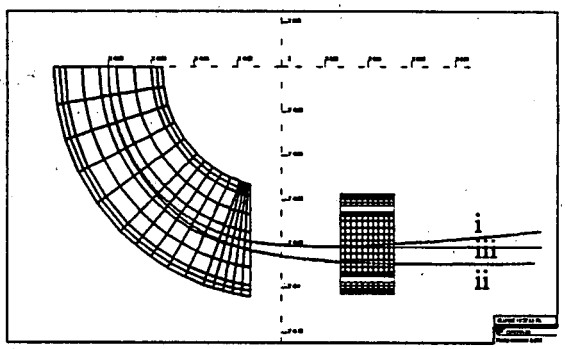

Figure 5 Alignment with different solutions

3 CONCLUSIONS

A finite element analysis of the ISIS H⁻ ion source analysing magnet has shown that with some design modifications a better alignment of the beam should be possible and the emittance benefits of operating at n=1 obtained. The design modifications requires the fitting of a 25 mm long tube separated from the pole by a gap of 36 mm ±5 mm and will be tested experimentally. There remains a residual offset which is greatly reduced by the tube arrangement. By allowing adjustment of the ion source in the vertical plane by ±2 mm it should be possible to align the source with the axis of downstream components. The combination of these two adjustments and the shielding effect of the tube should allow compensation for the mis-steering produced by the poles, without compromising the electron sweeping.

4 REFERENCES

1. Operational experience of Penning H⁻ Ion Sources at ISIS R.Sidlow this conference.
2. P.E.Gear and R.Sidlow Proc 2nd Inst Phys Conf Low Energy Ion Beams Bath 1980. Inst Phys Conf Ser No.54 P 284.

Acknowledgement.

The contribution of M.A.Clarke-Gayther with the development of the adjustable tube shielding concept is gratefully acknowledged.

PROGRESS OF THE RIST PROJECT

J R J Bennett, R A Burridge, T A Broome, C J Densham, P Drumm, W R Evans, I S K Gardner, M Holding, G M McPherson, G R Murdoch, V Panteleev*, and T G Walker,
CLRC's Rutherford Appleton Laboratory, Chilton, Didcot, Oxon OX11 0QX, UK
T W Aitken, J Kay, S Metcalf, H Price and D D Warner,
CLRC's Daresbury Laboratory, Daresbury, Warrington, WA4 4AD, UK
H Ravn, ISOLDE Group, CERN, CH-1211 Geneva 23, Switzerland

Abstract

The status and progress of the Radioactive Ion Source Test (RIST) Project [1] is given. A tantalum target consisting of nearly 6000 foils, 0.0025 cm thick, cut into discs and washers has been diffusion bonded together to form a rigid structure. In tests to date, 24 kW of power has been radiated from the finned surface at 2300 K.

1. INTRODUCTION

Future advanced radioactive ion beam facilities will require more intense beams than currently available. At the world leading ISOLDE facility [2], the radioactive beams are produced by the impact of high energy, 1 GeV, protons of up to ~2 μA on various targets. The RIST Project is aimed at the development of a high power tantalum foil target and ion source to produce higher intensity radioactive ion beams than are presently available at ISOLDE by bombardment with proton currents of up to 100 μA. The test is to be performed in the target station of the ISIS Facility [3]. The specific aims are:-

a) To produce a tantalum target which will withstand up to 100 μA of proton beam, corresponding to a power dissipation of 20 - 30 kW, depending on the detailed design. In addition, the target must be maintained at a uniform temperature of typically 2300 K.

b) To show that the radioactive beam currents are comparable with that from ISOLDE at the same proton current and scale with proton current.

c) To examine fluctuations of the high voltage on the target when the target is bombarded by intense pulsed proton beams.

2. TARGET CONSTRUCTION

The target is made from a stack of 0.0025 cm thick tantalum foil discs, spaced apart by washers. The thickness of the washers is adjusted to maintain uniform power dissipation along the length of the target. To dissipate the power by thermal radiation the thermal emissivity is increased by enlarging the

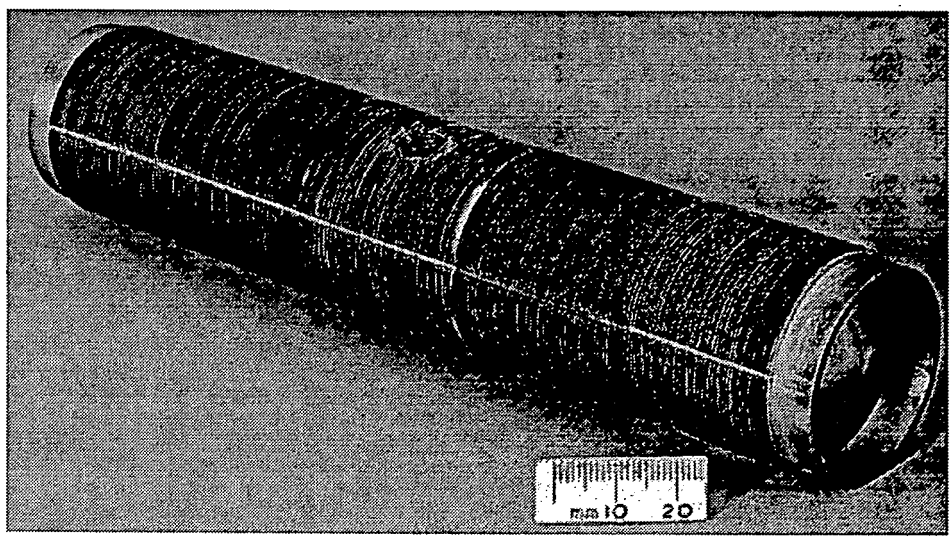

Figure 1. The diffusion bonded target assembly, with domed end caps and the central hole for the ioniser.

* On leave of absence from PNPI RAS, Gatchina, Russia

diameter of some of the discs to create fins, 0.1 cm high spaced at 0.03 cm intervals along the length of the target. The whole assembly, with dished end caps, is diffusion bonded together by pressing at 800°C in a vacuum to form a rigid gas tight structure, 18 cm long. Figure 1 shows a photograph of the completed target and Figure 2 shows a schematic cross section of the target construction.

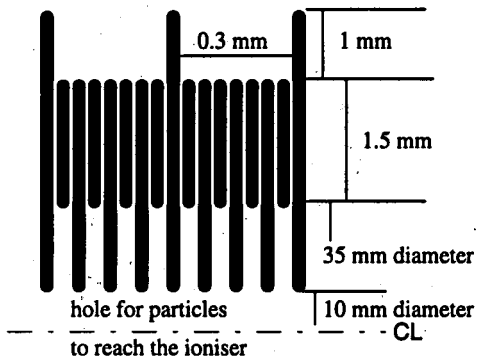

Figure 2. Schematic section of the target construction.

Seven tungsten wire filaments surround the target and provide electron beams to heat the target to the required temperature.

The target and the filament assembly are enclosed within a water-cooled copper jacket to remove the heat. Figure 3 shows the assembly schematically.

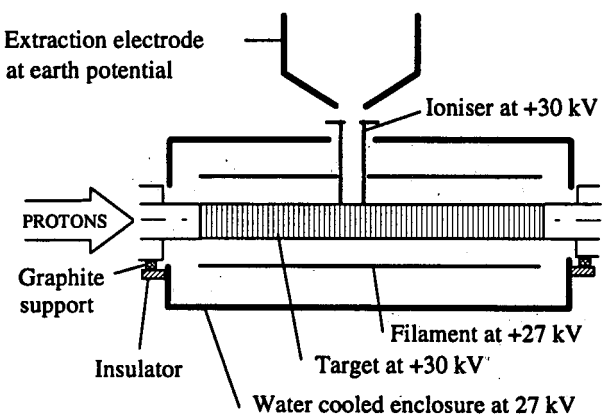

Figure 3. Schematic assembly diagram of target, ion source, filaments and extraction electrode.

3. THERMAL PERFORMANCE

The target has been heated by electron bombardment to a temperature of 2300 K at a power of 24 kW. This corresponds to a hemispherical total thermal emissivity of 0.72, the fins increasing the value by a factor of over 2 from that of a plain surface [4].

When the energy of the proton beam is dissipated in the target there will be radial temperature gradients across the foil discs and stresses set up in the target. To mimic this, a test section of target has been heated by an electron beam from a filament placed axially down the central hole. All the heat has to pass through the entire radius of the discs and this produces larger temperature gradients and stresses in the target than it will receive under normal proton beam bombardment. The diffusion bonds withstood this test up to the maximum specified power and temperature.

4. BEAM TESTS AT ISOLDE

Foil discs have been placed inside a standard ISOLDE target tube to simulate the RIST target geometry and the target run on ISOLDE at proton beam currents of up to 3 μA. The target was fitted with a standard tungsten ioniser. The yields of radioactive alkali metal and rare earth beams are comparable to those from the standard ISOLDE target. The release curves [5], which give the variation of the isotope current with time following a single proton pulse, are shown in Figures 4 and 5. The open squares are data from the standard ISOLDE target and the solid squares are from the RIST target. The vertical axis is

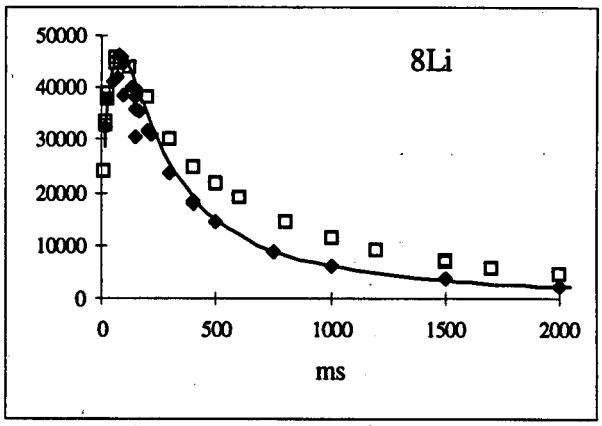

Figure 4. Release curve for ^{8}Li.

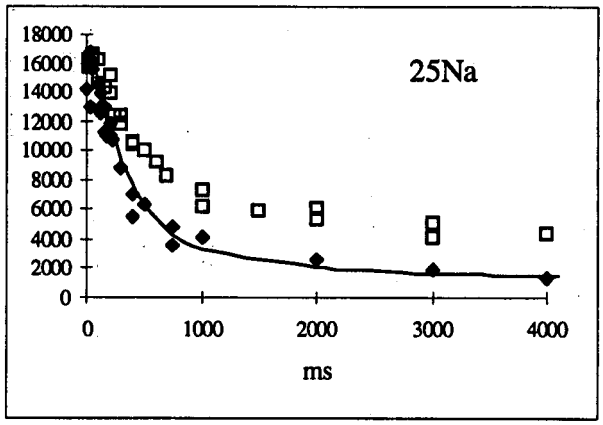

Figure 5. Release curve for ^{25}Na.

proportional to the isotope current: the data from the targets have been normalised at the peaks.

In general, the RIST target exhibits faster responses than the ISOLDE target. The ISOLDE target is filled with short rolls of tantalum foils and the faster response of the RIST target is probably due to its more open structure, which increases the effusion rate. This improvement will be important in increasing the yields of rare short lived isotopes.

5. HIGH VOLTAGE TESTS

When the target is bombarded by large pulsed proton currents the high voltage on the target may suffer from current loading problems and the voltage fluctuate. This is not acceptable for a high resolution separator.

To simulate the effects, the proton beam from ISIS has been passed through the walls of concentric tubular electrodes in a vacuum at potentials up to 30 kV. The vacuum is effective in eliminating the problem to negligible proportions. However, the insulation on cables adjacent to the beam gave rise to severe voltage fluctuations during the proton pulses. This is presumed to be due to ionisation of the insulation by the intense radiation. The voltage could be stabilised by the addition of a sufficiently large capacitor.

6. CONCLUSIONS

Thermal tests on the target are continuing, but already it has been demonstrated that the target is dissipating 24 kW at 2300 K. With an emissivity of 0.72 the target could probably dissipate up to 45 kW at 2700 K. Thus it has been demonstrated that the target is capable of dissipating well over 100 μA of proton beam current.

The tests of the target with proton beam at ISOLDE are very encouraging. The very short proton pulses at ISOLDE are similar in intensity to that of ISIS. Therefore, it is to be expected that the yields obtained from the RIST target at ISIS will be similar to those at ISOLDE at the same pulse proton beam current. Furthermore, the yields are expected to increase with the repetition rate. Thus the yield will scale with the proton current.

In addition the ISOLDE tests show that the geometry of the RIST target is likely to favour the production of the short lived isotopes by reason of its faster response times.

The high voltage tests show that loading from the beam hitting the target itself will not be a problem with the target in a vacuum. The ionization of neighbouring insulators can be overcome by the addition of suitable capacitance.

Thus, it can be concluded that the experiments have successfully met the goals of the RIST project even before running the target and separator on ISIS. Indeed, it is arguable whether a test at high beam power in the ISIS target station is now necessary.

7. REFERENCES

[1] J R J Bennett et al., Proceedings EPAC 94, 1415, 1994.

[2] H J Kluge (Editor), "ISOLDE Users Guide", CERN 86-05, 1986.

[3] J L Finney, "ISIS: A Resource for Neutron Studies of Condensed Matter", Europhysics News, vol. 20, (1989).

[4] A Sala, Radiant Properties of Materials, Elsevier, 1986.

[5] H L Ravn, S Sundell, L Westgaard and E Roeckl, Nucl. Instrum. Methods, **123**, 217, (1978).

DIPOLE AND QUADRUPOLE MAGNET DESIGNS FOR DIAMOND

N.Bliss, J.A.Clarke and N.Marks, CLRC, Daresbury Laboratory, Warrington WA4 4AD, UK;
M.R.Harold, CLRC, Rutherford Appleton Laboratory, Chilton, Didcot, Oxon, OX11 0QX, UK.

Abstract

As part of pre-design study investigations for the proposed synchrotron source DIAMOND, suitable magnetic and engineering configurations for the storage ring conventional dipoles and quadrupoles have been examined. The paper presents details of the current specifications for these magnets and possible designs that meet these requirements.

1 INTRODUCTION

Work is proceeding at the Daresbury Laboratory on a possible future UK synchrotron radiation source, DIAMOND [1]. This is currently specified as a third generation, 3 GeV storage ring light source, with full energy injection from a booster synchrotron. It is envisaged that the storage ring lattice may include super-conducting as well as conventional dipoles, functioning as the main lattice bending magnets. Whilst a full energy injector is being considered, the possibility of lower energy injection is not excluded at this stage; hence, the dipole design is required to provide adequate field quality between 1 and 3 GeV. The lattice also requires twelve different families of quadrupoles to provide the required control of the beta values in the achromats and at the insertion devices.

Work, resulting from a collaboration between the CLRC's two laboratories, on the design of the conventional dipole and the various quadrupoles is presented. In all cases, the magnetic field distributions shown have been predicted using the Vector Fields code OPERA 2D [2].

2 CONVENTIONAL DIPOLES

The conventional dipoles have the following specification:

number of dipoles (inc. s.c. magnets)	32 ;
minimum possible injection field	0.46 T ;
maximum field	1.4 T ;
required field homogeneity	$\pm 2 \times 10^{-4}$;
horizontal good field aperture	± 20 mm ;
magnet half gap at orbit	25 mm.

After a number of iterations, a pole geometry that substantially meets the required field quality was generated. A cross section through the pole is shown in Fig 1.

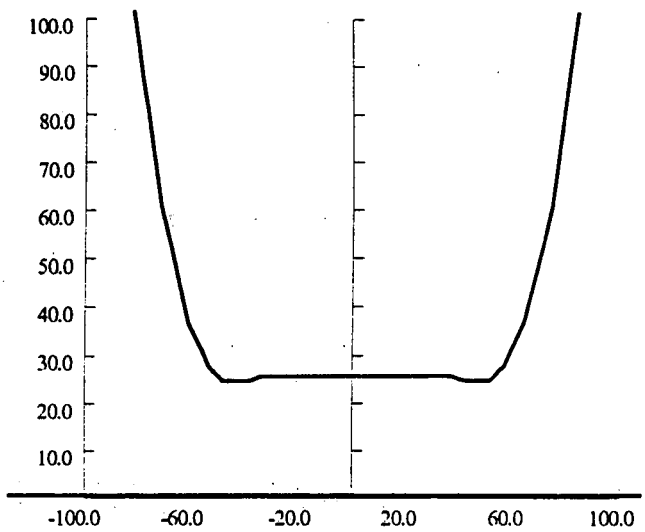

Fig 1: Pole geometry used for modelling the conventional dipole (dimensions in mm).

This pole geometry has the following parameters:

total pole width at root	180 mm ;
total pole width at shim	110 mm;
total shim width	20 mm;
shim height	0.9 mm.

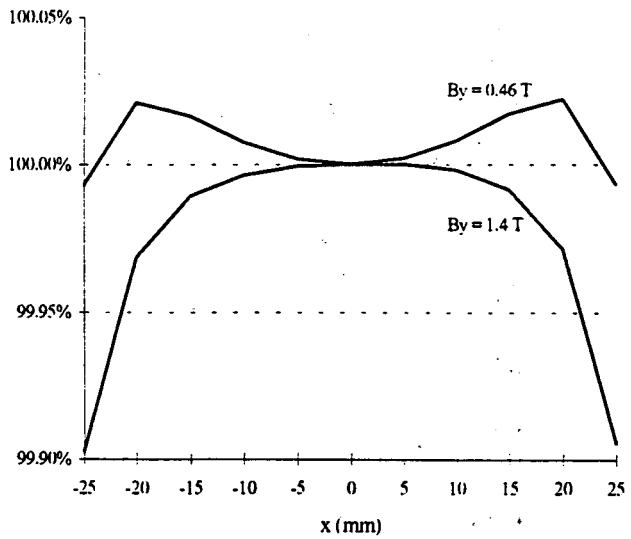

Fig 2: Homogeneity (%) of vertical field in the dipole as a function of horizontal position x.

The field quality predicted by OPERA 2D with non-linear steel (Magnetil BC) at both minimum and maximum fields is shown in Fig 2. It can be seen that the magnet meets the good field specification out to x = 18 mm at By = 1.4 T and exceeds the specification at the minimum field level.

3 QUADRUPOLE MAGNETS

The twelve quadrupole families have differing maximum strengths and, because of the variation of beam size through the lattice, differing aperture requirements. The relevant data is summarised in Table 1.

Table 1 Parameters for the twelve families of quadrupole magnet:

Fam.	Max. grad. T/m	No/ fam.	Hor. half app. mm	l m	R mm	Cross Sec.
Q 1	8.0	16	20	0.4	30	A
Q 2	20.0	16	20	0.6	30	B
Q 3	17.0	16	20	0.4	30	B
Q 4	8.0	12	20	0.4	30	A
Q 5	20.0	12	20	0.6	30	B
Q 6	17.0	12	20	0.4	30	B
Q 7	11.0	32	40	0.4	40	C
Q 8	15.0	32	40	0.4	40	C
Q 9	8.0	4	25	0.4	30	A
Q 10	12.0	4	25	0.6	30	B
Q 11	15.0	4	25	0.6	30	B
Q 12	8.0	4	25	0.4	30	A

Good gradient is currently defined as:

$$\Delta g / g (0) \leq 0.05\%.$$

In addition to giving the maximum required quadrupole gradient, the number of magnets per family, the required good gradient half aperture and the magnetic length, the sixth column of the Table also gives the minimum possible inscribed radii, determined from preliminary estimates of vacuum vessel dimensions.

A requirement to maintain a minimum clearance for emerging beam-lines in the regions of the pole and coil corners applies an additional constraint:

minimum allowed vertical pole and coil clearance = ± 10 mm.

The use of a different cross section design for each family would be highly uneconomic and therefore it is proposed to use only three quadrupole cross sections to accommodate all twelve families, there being different magnet lengths needed in some cases; the last column in Table 1 gives the cross section that is proposed for each family. Work on each of these cross sections is presented below.

3.1 Cross section A.

Cross section A is a low gradient magnet with a conservative good gradient aperture of 20 mm; little difficulty was encountered during the design work. Using a hyperbolic pole with a linear tangential shim commencing at:

x = 32.5 mm y = 13.85 mm

and terminating at:

x = 41.53 mm y = 10.00 mm

good quality gradient was obtained across the specified aperture. The gradient homogeneity is shown in Fig 3.

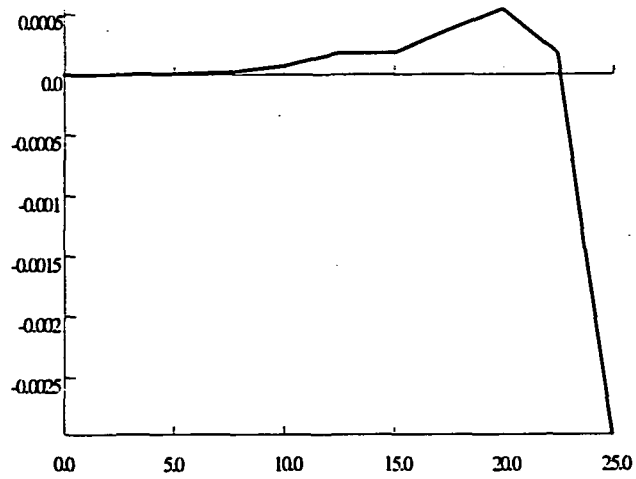

Fig 3: Fractional variation in gradient with horizontal position x (mm) on the y = 0 axis in the cross section A quadrupoles at a gradient of 16 T/m.

3.2 Cross section B.

This cross section has higher maximum gradient of 20 T/m and, in the case of families 10 and 11, a larger good gradient aperture of 25 mm. Difficulties encountered during the design included high flux densities at the pole root, which led to non-linear behaviour, and problems in obtaining the required gradient aperture without infringing the minimum specified pole clearance of 10 mm. A geometry that overcomes these difficulties is shown in Fig 4, the diagram showing one eighth of the total quadrupole.

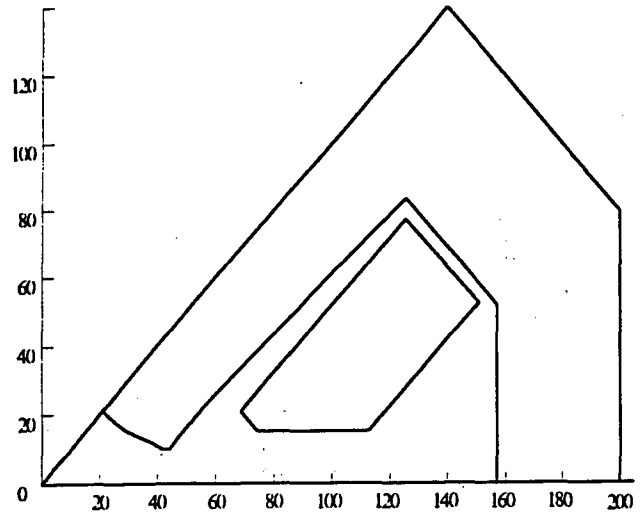

Fig 4: One eighth pole geometry for the quadrupole cross section B (dimensions in mm).

The hyperbolic pole is terminated by a linear shim commencing at:

x = 38.000 mm y = 11.842 mm;

and terminating at:

x = 41.800 mm y = 10.000 mm;

followed by a horizontal section, terminating at:

x = 44.000 mm y = 10.000 mm.

This horizontal section of the pole was found to be effective in extending the good gradient region, without infringing the region below y = 10mm. Additionally, the pole is thickened at the root, overcoming the problem of non-linearities. The predicted gradient quality for this geometry at g = 20 T/m, with non-linear, Magnetil BC steel, is shown in Fig 5.

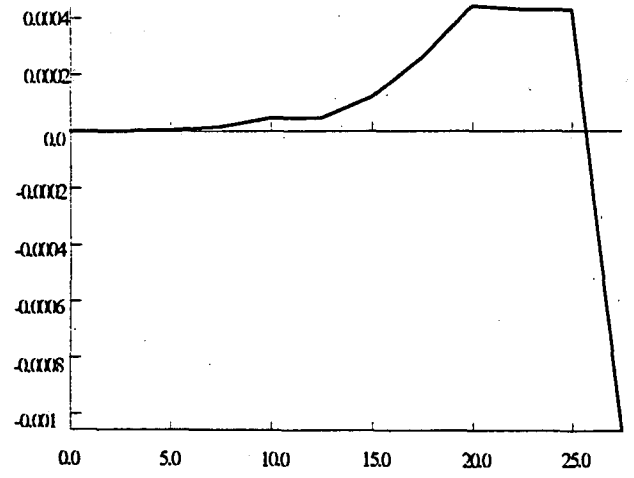

Fig 5: Fractional variation in gradient with horizontal position x (mm) on the y = 0 axis in the cross section B quadrupoles at a gradient of 20 T/m.

3.3 Cross section C.

It was found to be possible to obtain the full 40mm good gradient aperture with the 40mm inscribed radius by using a linear shim commencing at:

x = 53.000 mm y = 15.094 mm

and terminating with the pole corner at:

x = 66.000 mm y = 11.392 mm.

The predicted gradient quality at 15 T/m with non-linear steel for this geometry is shown in Fig 6.

It can be seen from the figure that the inscribed radius of 40 mm helps to establish a larger good gradient region without infringing the 10 mm clearance.

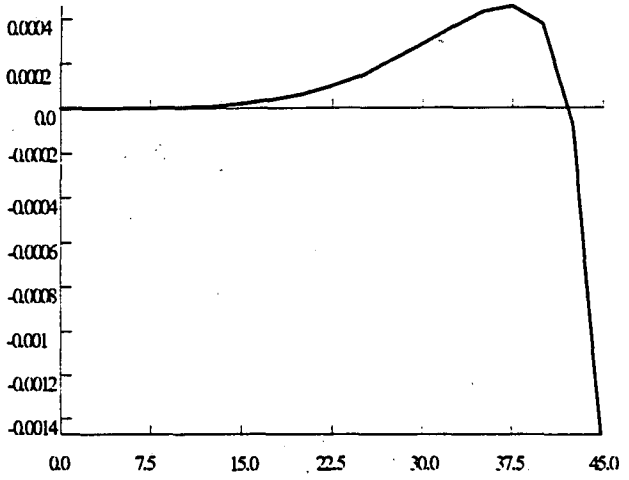

Fig 6: Fractional variation in gradient with horizontal position x (mm) on the y = 0 axis in the cross section C quadrupoles at a gradient of 15 T/m.

4 CONCLUSION

The work reported represents an initial examination of the quadrupole arrangements for DIAMOND. This information can now be used for more detailed examinations of the engineering layout of the lattice and for the assessment of field and gradient quality using particle tracking programmes. Further refinements and adjustments are then expected.

REFERENCES

[1] 'Further Design Progress on DIAMOND, the Proposed New UK National Light Source', M.W. Poole and V.P. Suller, these Proceedings.

[2] Produced by Vector Fields Ltd., 24 Bankside, Kidlington, Oxford OX5 1JE, UK

STRIPPING FOIL TEMPERATURES IN THE EUROPEAN SPALLATION SOURCE

Jonathan Duke,Rutherford Appleton Laboratory,Chilton,Didcot,United Kingdom.

1 INTRODUCTION

Aluminium oxide (Al_2O_3) and graphite have been studied as possible stripping foil materials as part of the ESS study. The ESS is a next generation neutron source and designed to use H^- injection (1).This report describes the study of projected foil temperatures which has been carried out. The foil is to be rectangular, 22.1 mm wide and 13.3 mm high, supported only on two sides to reduce the number of subsequent foil transits by recirculating protons. A foil mass per unit area of 345 $\mu g\ cm^{-2}$ was chosen, corresponding to a thickness of 1.275 μm for Al_2O_3 and 2.247 μm for graphite. The H^- beam is centred 6.4 mm from the open foil corner and has an elliptical transverse boundary with radial and vertical beam semi-axes of 2.45 and 2.10 mm respectively. Other relevant input parameters are a 1000 turn injected beam of 2.34 10^{14} ppp at a repetition frequency of 50 Hz and with a pulse duration of 600 μs.

Injected H^- ions, stripped electrons and recirculating protons scatter in the foil and large temperature rises result from atomic excitations and ionisation. The initial rate of temperature rise is inversely dependent on the foil specific heat. The temperature reaches a maximum at the end of injection and the temperature rise in the 50 Hz cycling is limited mainly by radiation, with a small additional contribution from conduction within the foil. A constant peak temperature is reached after approximately five beam pulses. Power losses due to radiation and conduction scale as the fourth and first power of the temperature difference from the surroundings, and are proportional to the foil emissivity and thermal conductivity respectively. The specific heat, emissivity and thermal conductivity are all material and temperature dependent.(2),(3).

2 SIMULATION

Heating and cooling of the ESS foil have been simulated in a program based on finite elements, both for time elements and transverse position co-ordinates. Radial and vertical dimensions have been scaled in the ration of 5:3 to give approximately square elements, with 50 radial elements and 30 vertical elements. The distribution of recirculating protons on the foil was based on the injection tracking studies, and the data was input to the program as the charge incident on each element per turn.This was estimated by scaling the integrated charge by the size of the recirculating beam in the ring at each time point. In reality the recirculating proton hits do not have a simple time distribution, but the use of an approximation was justified by the savings made in memory and computer time. Energy deposited in the foil is calculated using charged particle energy loss data, both for protons and stripped electrons.(4),(5). For the H^- ions, one electron was assumed to strip on entry to the foil, and the other at the midpoint. High temperature estimates for specific heat have been made by scaling normalised Debye curves (6) in both dimensions to give a best fit for published data. Asymptotes used for the specific heats at high temperatures are 1289.3 and 2125 $Jkg^{-1}K^{-1}$ for Al_2O_3 and graphite respectively. Emissivities were kept constant at 0.4 for Al_2O_3 and 0.825 for graphite. Thermal conductivities were approximated by:

$4.765 + 2664470\ T^{-1.9496}$ for Al_2O_3.
$15 + 305958\ T^{-1.3091}$ for graphite with $T > 573$ K and
$217.9653 - 0.2233\ T$ for graphite with $T < 573$ K.

By altering independently the input parameters such as emissivity, heat capacity, the time distribution of hits by recirculating protons and the energy dumped in the foil by one proton , the variation in modelled foil temperatures caused by the uncertainties in the input conditions was calculated.The most important uncertainty is in the emissivities - this is largest for Al_2O_3. When all the variations due to varying input conditions are summed, the total estimated uncertainties in peak equilibrium temperatures are:
Al_2O_3 : $+5.3\% -11.5\%$. Graphite : $+1.3\% - 2.0\%$.

The peak temperature in the graphite foil is 2380 K, while that in the Al_2O_3 foil is 3083 K. These should be compared to melting points of 3823 K for graphite but only 2320 K for Al_2O_3 . The difference in temperature is due to graphite's larger emissivity and specific heat . It is possible that the emissivity of Al_2O_3 may rise with temperature, but even if ε approached 1.0, this would only reduce the temperature to 2745 K, still well above the melting point. The results of the simulation are shown below in Figures 1-4 for the condition just after the passage of the fifth beam pulse. The higher thermal conductivity of graphite has caused the lower contours to spread out much further in the same period., but the effect of this on the peak temperature is insignificant - (~ 0.1 K.)

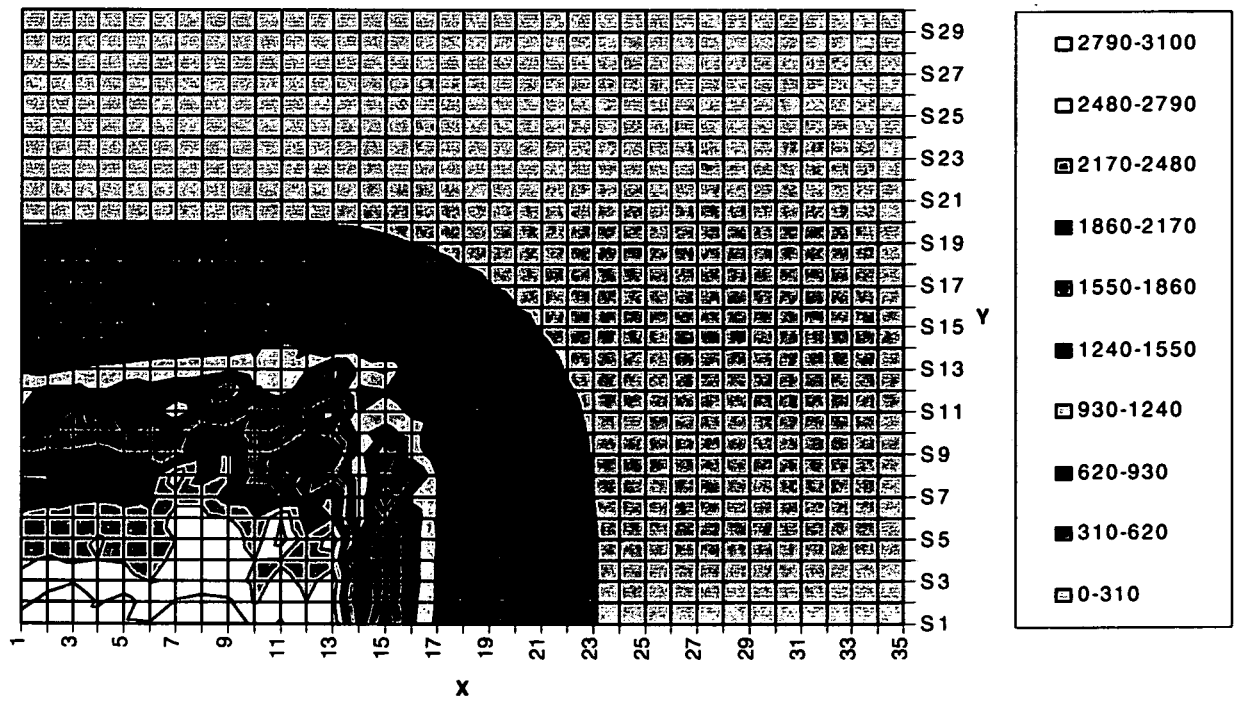

Figure 1 Contour plot of Aluminium Oxide Stripping-foil temperatures (K)

SCALE In all figures: X Division= 0.4427 mm, Y Division= 0.4435 mm

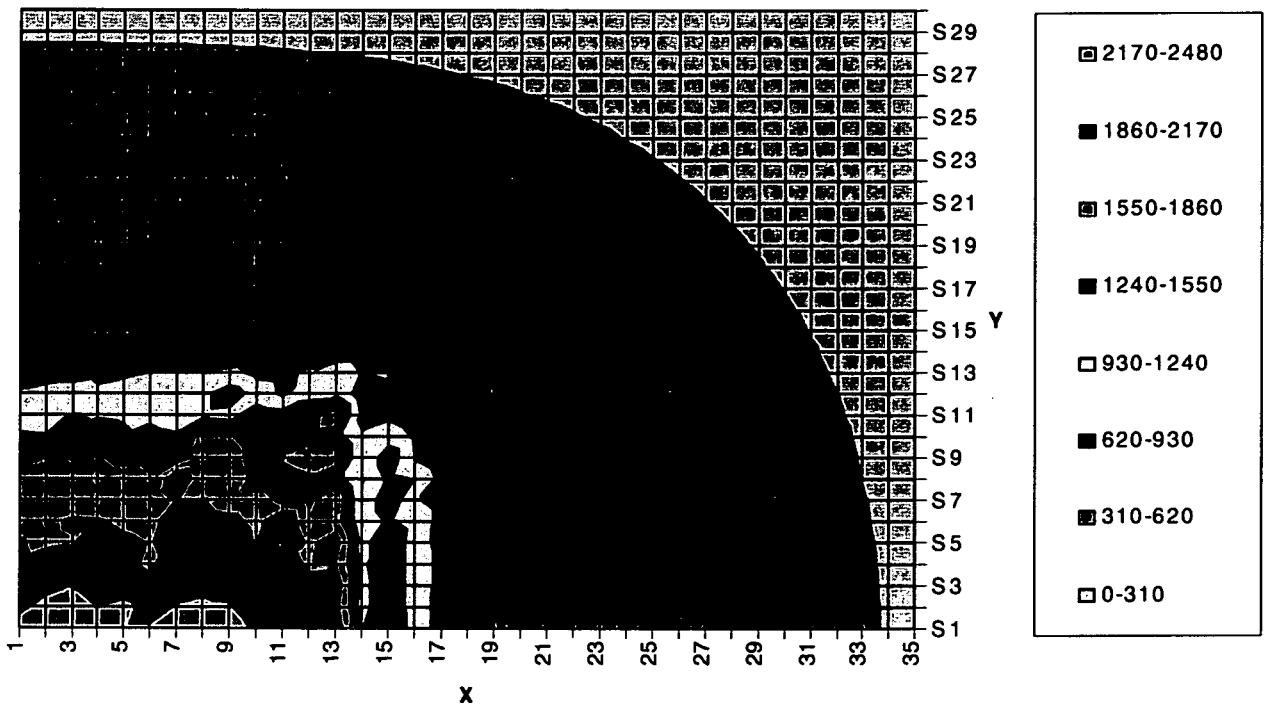

Figure 2 Contour plot of Graphite Stripping-foil temperatures (K)

3 CONCLUSION

It is therefore apparent that graphite is the better material for ESS foils. It is also evident that foils may set performance limits for the ESS , and that the foil performance required is at least equivalent to that achieved with the INS Carbon foils made by the'mCADAD' method (7) and tested in the Proton Storage Ring at LANL.

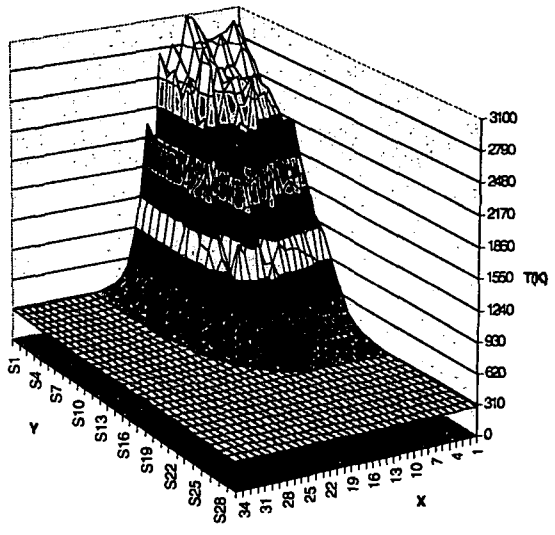

Figure 3 Aluminium Oxide Stripping-foil Temperature Profile

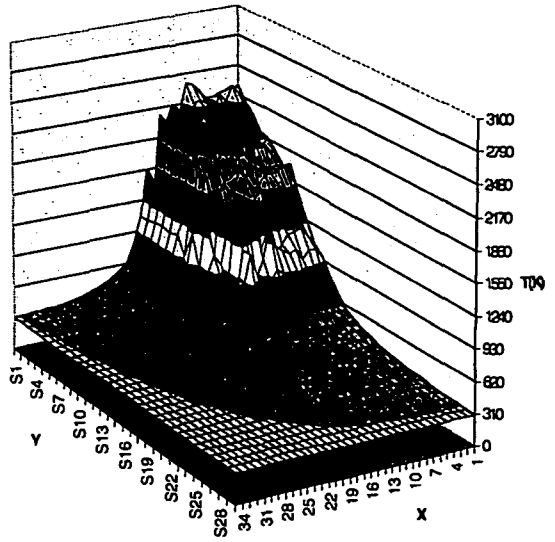

Figure 4 Graphite Stripping-foil Temperature Profile

REFERENCES

(1) I.S.K.Gardener et al, editors
'Outline Design of the European Spallation Neutron Source'. report no. ESS 95 30-M
pp. 3.8-3.9

(2) Arthur M. James and Mary P.Lord
'Macmillan's Chemical and Physical Data'
- pub. The Macmillan Press Ltd. 1992
pp. 40,434,438,442

(3) Y.S Touloukian and D.P.Dewitt
'Thermophysical Properties of Mattter -Vol.8- Thermal Radiative Properties - Nonmetallic Solids'
pub. IFI / Plenum ,New York. 1972 pp. 31,142-3

(4) J.F. Kanni,Kirtland Air Force Base, New Mexico.
Atomic Data and Nuclear Energy Tables-
Proton Range-Energy Tables , 1 keV-10 GeV
Volume 27 Numbers 2/3
Academic Press, 1982. p. 219

(5) Subcommittee on Penetration of Charged Particles and Committee on Nuclear Science
Nuclear Science Series -Report no. 39
'Studies in Penetration of Charged Particles in Matter'
publication 1133 , National Academy of Sciences-National Research Council, USA. 1964
pp. 232,234,237,146

(6) Mark W Zemansky and Richard H Dittman
'Heat and Thermodynamics' (sixth edition)
pub. Mcgraw-Hill Book Company. 1981 pp. 309-11

(7) Dr I. Sugai et al
'Development of thick, long-lived carbon stripper foils for PSR of LANL'
' Nuclear Instruments and Methods in Physics Research' - Section A ,no. 362 (1995), p.70

A HIGH STABILITY INTENSITY MONITORING SYSTEM FOR THE ISIS EXTRACTED PROTON BEAM

Michael A. Clarke-Gayther, RAL, Didcot, United Kingdom

ABSTRACT

A description is given of the extracted proton beam intensity monitoring system on the high intensity pulsed neutron source, ISIS, at the Rutherford Appleton Laboratory. The system, consisting of six resonant mode toroidal beam current monitors, and signal conditioning electronics, measures protons per pulse in the range 2e10-4e13 p.p.p. with good linearity, and has shown excellent long term stability.

1 INTRODUCTION

The non-destructive, accurate, and stable measurement of beam intensity is an important diagnostic requirement at particle accelerators. Measurement systems, based on toroidal beam current transformers [1], where the charged particle beam, and its image (wall) current form a single turn primary winding, are in widespread use, and have been the subject of continuous development [2]. High accuracy AC, DC, and DC to wide-band beam transformers are now commercially available [3]. Systems can be configured to provide information on: the time dependent variation of beam current (current viewing); the instantaneous beam current (sampled); the average beam current; and the beam charge (charge per pulse). Processed measurements yield data on accelerator system efficiencies (e.g. at injection, acceleration or extraction), and beam loss.

Accurate measurement of beam charge for beam pulse durations in the 1e-8 to 1e-5 (s) range has been demonstrated by systems using integrating resonant mode beam transformers [4,5]. A system of this type, consisting of six resonant mode toroidal beam current transformers, and signal conditioning electronics, measures protons per pulse, in the extracted proton beam at ISIS.

2 THEORY OF OPERATION

The equivalent circuit for the generalised beam current transformer is shown in fig.1. The pulsed beam current I_B and its image (wall) current form a single turn primary winding, inducing a magnetic flux Φ in the core and a voltage V_s across the secondary winding. The high permeability toroidal core ensures tight magnetic coupling (k=1) between the primary and secondary windings.

Where: $V_S = -kn\dot{\Phi} = -knL_0\dot{I}_P = -kL_S\dot{I}_P/n$ is Faraday's law, $I_P = I_B$, and L_0, L_S, R, C, and n, represent the single turn inductance, the total secondary inductance, the total losses, the secondary load capacitance and the number of secondary turns.

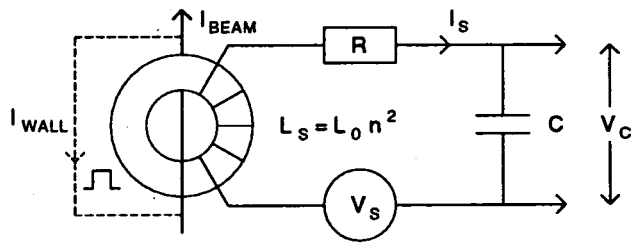

Figure 1: Equivalent circuit of beam current transformer

The voltage loop equation, describing the transfer function of the equivalent circuit, is given by:

$$L_S\dot{I}_S + RI_S + Q_C/C = -kn\dot{\Phi} = -kL_S\dot{I}_P/n$$

with the general solution of the homogeneous equation given by:

$$I(t) = c_1e^{-\lambda_1 t} + c_2e^{-\lambda_2 t}, \quad \lambda_{1,2} = \frac{R}{2L_S} \pm \sqrt{\frac{R^2}{4L_S^2} - \frac{1}{L_SC}}$$

There are two important cases:

1. When: $\frac{R^2}{4L_S^2} - \frac{1}{L_SC} > 0$, (overdamped response)

λ_1 and λ_2 are real, and the response is that of the simple current transformer, with a time constant $\tau = L_s/R$, and where $I_s = I_B/n$. Electronic integration of I_s can provide a measure of charge, but this process can be inaccurate for short pulses.

2. When: $\frac{R^2}{4L_S^2} - \frac{1}{L_SC} < 0$, (underdamped response)

λ_1 and λ_2 are complex, and the response is that of the resonant mode transformer, where the secondary current charges load capacitor C during the beam pulse, and initiates a damped oscillation at the natural resonant frequency ω_0 of the LCR network. The amplitude of the oscillation, sampled as the voltage developed across C, can be shown to be proportional to beam pulse charge. This relationship is explored, without loss of generality, by analysing the solution of the loop equation for a gate function beam current pulse of duration T.

Where: $I_P(t) = I_B$ for $0 \le t \le T$
and, $I_P(t) = 0$ for $t > T$,

the exact solution for V_c (t) can be shown [5] to be given by the sum of two exponentially decaying sine functions, initiated at t = 0 , and at t = T, respectively, as shown in fig.2, giving:

$$V_C(t) = -\frac{I_B}{n\omega_0 C} e^{-\lambda t}\left[(\sin\omega_0 t) - (e^{\lambda T}\sin\omega_0(t-T)_{t\geq T})\right]$$

where the resonant frequency: $\omega_0 = \sqrt{\frac{1}{L_S C} - \frac{R^2}{4L_S^2}}$

and the decay time constant: $1/\lambda = 2L_S/R$

Figure 2: Exact solution functions for V_c (t)

$$\text{As } T\to 0 \qquad V_C(t) \approx \frac{-2I_B}{n\omega_0 C}(e^{-\lambda t}\cos\omega_0 t)$$

and for T>0, and $\lambda < 0.01\omega_0$ the following simplified equation gives a value for $V_c(t)$ that is in error by < 0.01% of the exact solution:

$$V_C(t) \approx \frac{-2I_B}{n\omega_0 C}\left[\sin\frac{\omega_0 T}{2}\right]\left[e^{-\lambda(t-T/2)}\right]\left[\cos\omega_0\left(t-\frac{T}{2}\right)\right]$$

$$\text{For } \omega_0 T < 1, \quad \sin\omega_0 T \approx (\omega_0 T/2 - \omega_0{}^3 T^3/3!2^3)$$

$$V_C(t) \approx \frac{-I_B T}{nC}\left[1-\frac{\omega_0{}^2 T^2}{24}\right]\left[e^{-\lambda(t-T/2)}\right]\left[\cos\omega_0\left(t-\frac{T}{2}\right)\right]$$

where the terms in brackets are due to: integration error, damping, and waveform function, respectively. For beam pulse durations in the range $0 < T \leq T_{MAX}$ the magnitude of the corresponding integration error Δ (%) is determined by the resonant frequency ω_0 , where: Δ (%) = ($\omega_0{}^2$ T^2/24) 100.

Finally, if V_c is sampled at t = ((π/ω_0) + T/2), and the beam pulse duration (T) is a constant (as is the extracted beam pulse at ISIS), the contributions from the pulse duration dependant terms can be combined giving:

$$V_C(t) \approx \frac{I_B T}{nC}(A) \approx \frac{Q_B}{nC}(A)$$

Where Q_B is the total beam pulse charge, and A is a unique calibration constant, determined for each channel.

3 MECHANICAL DESIGN FEATURES

The mechanical construction of the resonant mode current transformer is shown in fig.3. This UHV compatible, radiation hard design, occupies a minimum beamline length, and utilises an ex-RF cavity, nickel-zinc ferrite core (μ_R = 180), with a 50 turn, centre tapped secondary winding. A nickel plated steel casing, with an internal mumetal screen provide isolation from interfering magnetic and electric fields. The precision (NPO) ceramic chip, load capacitor(s) [6] are mounted on a plug in printed circuit board that can be easily removed for measurement purposes. The housing is fitted with 'quick release' vacuum, and mounting clamps, to facilitate efficient 'hands on' maintenance.

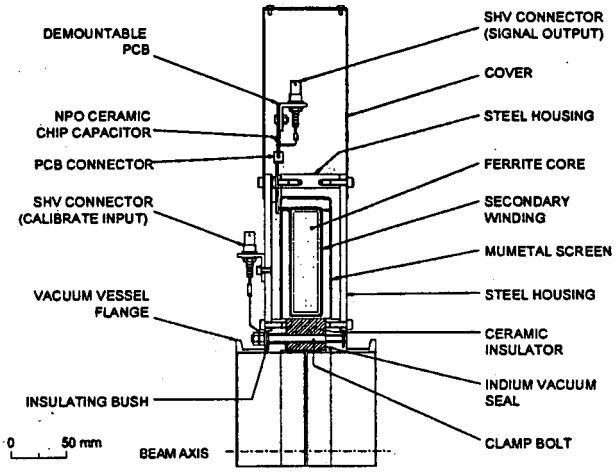

Figure 3: Beam transformer construction

4 ELECTRONIC SYSTEM DESIGN

The important features of the signal conditioning and data acquisition system are shown in fig.4. Values for the secondary inductance (L_s), number of turns (n), and load capacitance (C), were chosen to give an

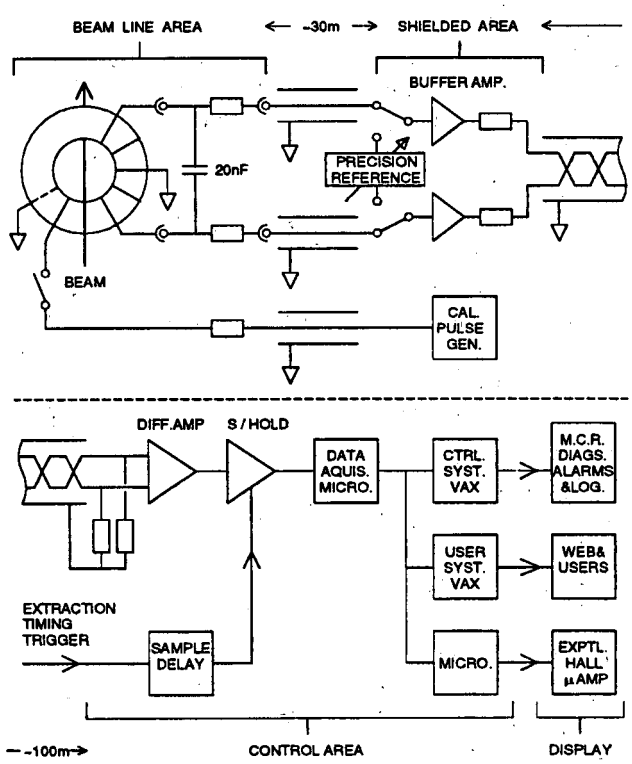

Figure 4: Electronic system schematic

acceptable compromise between signal amplitude, frequency (ω_0 / 2π), integration error (Δ), and damping factor (λ). The ISIS resonant mode beam transformers have the following design parameters:

ω_0 = 1.9e5 s^{-1}	n = 50	μ_R = 180
L_S = 1.4e-3 H	C = 2e-8 F	R = 1.8 Ω
Δ = 0.02 %	T = 4.0e-7 s	1/λ = 1.5e-3 s

The secondary winding outputs a balanced differential signal, with a dynamic source impedance of ~ 40 kΩ, to a remote, high impedance buffer amplifier, via ~30 metres of low capacitance coaxial cable. The capacitance of this cable, forms part of the total load capacitance, and is included in the calculated channel calibration constant. The buffered, high level, low impedance signal, is output to a remote differential receiver amplifier, via ~100 metres of screened, twisted pair cable. A delayed timing pulse, synchronised to beam extraction, triggers a precision sample-hold circuit that subsequently acquires and stores the transformer signal, at peak amplitude, during the first cycle of oscillation. A schematic of the primary and secondary

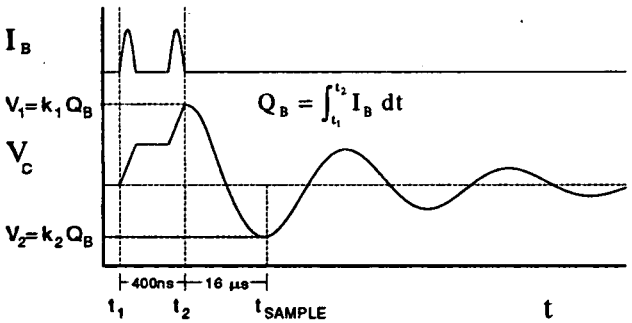

Figure 5: Waveform schematic

waveforms is shown in fig.5, where $V_C = V_1$ at the end of integration, and $V_C = V_2$ at the peak of the first maximum. The signal decays with a time constant of 1.5 ms (Q = 140), and drops to < 1e-6 of the initial value in the ISIS cycle time of 20 ms. The six sampled signals are digitised, and the resulting raw data is distributed to the display systems as shown in fig.4.

5 TEST SET-UP

The relationship between transformer primary charge, and secondary voltage was determined using the circuit shown in fig.6. The circuit simulates the ISIS extracted beam pulse. A charged line (Z_0 = 12.5 Ω), with a precisely determined electrical length (400ns), delivers a pulse with a programmable voltage amplitude in the range 0.1 ~ 100 V, to a precision high voltage, pulse rated termination [7], resulting in a primary charge pulse in the range 3e-9~3e-6 C. The secondary voltage waveform, sampled at the first maximum, divided by the primary pulse charge ($Q_P = V_L T_P$ / 2 Z_0), yielded a

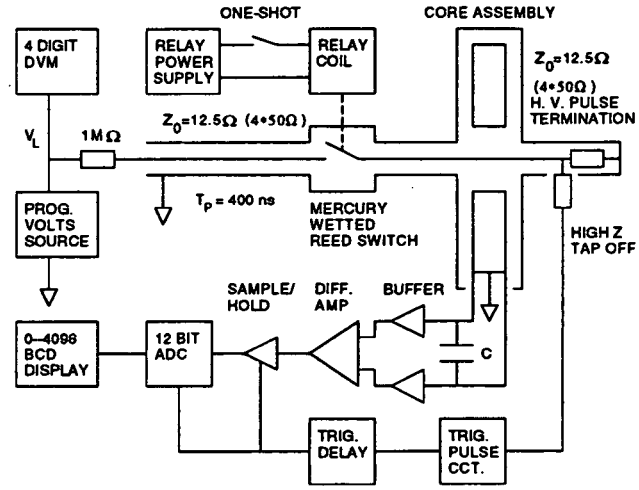

Figure 6: Test circuit schematic

measurement of non-linearity of ± 0.2% for primary charge in the range 3e-9~ 3e-6 C. The accuracy of calibration was estimated to be within 0.5 % of absolute.

6 OPERATIONAL EXPERIENCE

The resonant mode beam charge monitoring system has demonstrated excellent long term calibration stability. The calibration factors for the six transformers have changed by < ± 0.1% / year. The precision ceramic chip capacitors, have been measured at regular intervals, and show changes in value of < ± 0.01% year, including, in one case, a component that has received an estimated accumulated radiation dose of between 3e5 and 5e5 Gy.

7 ACKNOWLEDGEMENT

Contributions from the following are gratefully acknowledged. A. Borden, and D. Wright (data acquisition microcomputer, software and display), R. Steiner (helpful comments), M. Southern (mechanical design), ISIS Controls group (display hardware and software), and many others.

REFERENCES

[1] Robert C. Webber, 'Charged Particle Beam Current Monitoring', AIP conf. proc. No.333 (1995), p.3-23.
[2] Klaus B. Unser, 'Recent advances in beam current transformer technology', Proc. of first European workshop on beam diagnostics, Montreux, Switzerland, May 1993, p.105-109.
[3] Julien Bergoz,'Current monitors for particle beams', Nuclear Physics, A525 (1991), p.595c-600c.
[4] R. Steiner, K. Merle and H. G. Andresen, 'A high-precision ferrite-induction beam-current monitoring system', Nucl. Instr.and Meth. 127 (1975), p.11-15.
[5] R. S. Larsen and D.Horelick, 'A precision toroidal charge monitor for SLAC', SLAC-PUB-398 (1968).
[6] Vitramon Ltd, High Wycombe, Bucks., UK.
[7] Barth Electronics Inc., Boulder City, Nevada, USA.

STABILISING THE VOLTAGE OF THE DC ACCELERATING COLUMN OF THE ISIS PRE-INJECTOR USING A BEAM CURRENT CONTROLLED 'BOUNCER'

M. Perkins, V.C. Cloke, Rutherford Appleton Laboratory, Chilton, Didcot, Oxon, U.K.

ABSTRACT

To prevent the EHT supply tripping on overcurrent after an electrical discharge in the accelerating column and thus allow rapid recovery of the accelerating potential, the limiting resistor value has been increased. This resistor which connects the reservoir capacitor to the high voltage platform has been changed from 10kΩ to 1MΩ. The now excessive sag on the accelerating voltage, resulting from beam loading is compensated by 'bouncing' the voltage at the base of the reservoir capacitor. The Bouncer, operating in an extremely electrically hostile environment is fully remote controlled with automatic control of the Bouncer pulse provided by feedback from a beam current toroid. The paper describes the design of the system and covers such factors as reliability, electrical safety interlocking and oil cooling as well as satisfying the required performance specifications.

1 INTRODUCTION

On the ISIS pre-injector H^- ions are accelerated from the ion source by a 665 kV negative DC potential, generated by a 10 stage Cockcroft-Walton type multiplier. During the beam pulse the accelerating potential, under the influence of beam loading, tends positive by a value proportional to the value of a current limiting resistor between a reservoir capacitor and the ion source platform. The accelerating column has suffered from repeated electrical breakdowns that trip the EHT power supply on overcurrent. The incidence of spurious breakdowns has been reduced to about ten a day on average.

To minimise ISIS beam off time the susceptibility to breakdowns of the power supply has been reduced and the recovery time shortened considerably. The main factor in reducing the susceptibility to breakdown has been the factor of ten increase in the current limiting resistor value.

The increase in the current limiting resistor resulted in too much energy spread in the accelerated beam due to the larger potential droop produced by the beam loading. The ISIS pre-injector 'Bouncer' has been developed as a method of stabilising the accelerating potential against the effects of beam loading.

2 BOUNCER PULSE AMPLIFIER

2.1 EHT Circuit

The circuit of the EHT supply is shown in Figure 1. The beam pulse removes electric charge from the reservoir capacitor through the new 1MΩ current limiting resistor. This can be restored by 'bouncing' the base of the reservoir capacitor with a negative going pulse. The amplitude, shape, width and position in time of the pulse determines the stability of the accelerating potential.

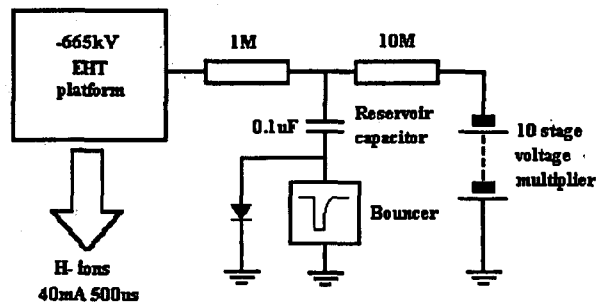

Figure 1 - EHT power supply circuit

2.2 Bouncer output stage

The heart of the system is a high voltage pulse amplifier that uses a Thomson TH5184 oil cooled tetrode [1]. At an anode voltage of 60 kV and 50 Hz repetition rate. This gives a maximum output pulse capability of 55 kV for 330 μs without exceeding the maximum anode dissipation of 1 kW. The tube is mounted in a electrically and mechanically interlocked oil filled container that also contains the main components of the output stage along with earthing and energy dumping switches. The output is capacitively coupled to a base plate on the reservoir capacitor with a high voltage diode to prevent positive excursions and a spark gap to protect the amplifier. Resistor chains provide a high impedance path from the plate to ground to bias the base-plate.

2.3 Power supplies

All the power supplies for the system are mounted in a 19" rack adjacent to the pulse amplifier tank in the ISIS

pre-injector EHT area. The TH5184 control grid bias, screen grid bias and anode power supplies are commercial units with remote control/monitor facilities. Filament power to the tetrode is from an in house designed 7.2 V ±2% at 20A voltage regulated supply. This has automatic ramp-up capability with overcurrent and monitoring facilities as integral features. The filament regulator also controls the main power interlocks.

2.4 Drive signal and feedback

The Bouncer can be driven in two modes, manual or automatic. In the manual mode, a pulse of adjustable amplitude is sent to the grid driver unit. The timing of this gate pulse is also adjustable from the main control computer. The platform voltage sag can be tuned out by using the platform voltage signal as a reference. In automatic mode the output from a beam current toroid immediately downstream of the dc accelerator is used to give a signal that is related to the charge drain on the reservoir capacitor. The use of negative feedback removes the need to adjust the gain and pulse parameters. A differential signal is used to transport the drive pulse the 100 metres to the control grid driver unit, which is in the forward path of a local negative feedback loop from the bouncer output. This sets the gain of the amplifier and reduces the susceptibility to oscillation. Feedback is provided from a commercial potential divider, which also provides an output monitor signal.

2.5 Controls

The Bouncer system has been designed to be simple to operate, having only one button for switch on in normal running conditions. Operation of the switch automatically opens the energy dump relay and all the supplies are automatically and sequentially switched. Remote indication of power supply settings and interlock status are provided and a signal patching network is included for remote diagnostics.

2.6 Interlocking and safety

The system is interlocked for both personnel safety and correct method of operation by both electrical and mechanical systems. Shutting down the equipment automatically operates energy dissipation and charge leakage systems.

Access to the oil bath for inspection or tube replacement can only be achieved with all earthing devices ON and the main power supplies OFF. A 'key' operated test facility allows local operation of the system, but special safety precautions must be observed.

2.7 Oil cooling

The oil filled container has a capacity of $1m^3$ (~ 1 tonne) of insulating transformer oil, which is temperature regulated to around 30° C using a ring of water cooled pipes around the top of the container. A pumping system drains the oil into a separate compartment of the tank for tube changing and repair purposes. The container stands in a bund large enough to contain the oil in the event of a leak.

3 PERFORMANCE AND RELIABILITY

3.1 Performance

Installation of the new current limiting resistor has significantly reduced overcurrent trips of the EHT power supply on voltage breakdown. This allows automatic recovery of the accelerating potential in ~70 ms. The loss of only three beam pulses per breakdown has dramatically improved the availability of ISIS.

Stabilisation of the platform potential to within ± 2 kV during the beam pulse is achieved to compensate the consequential effects of beam loading.

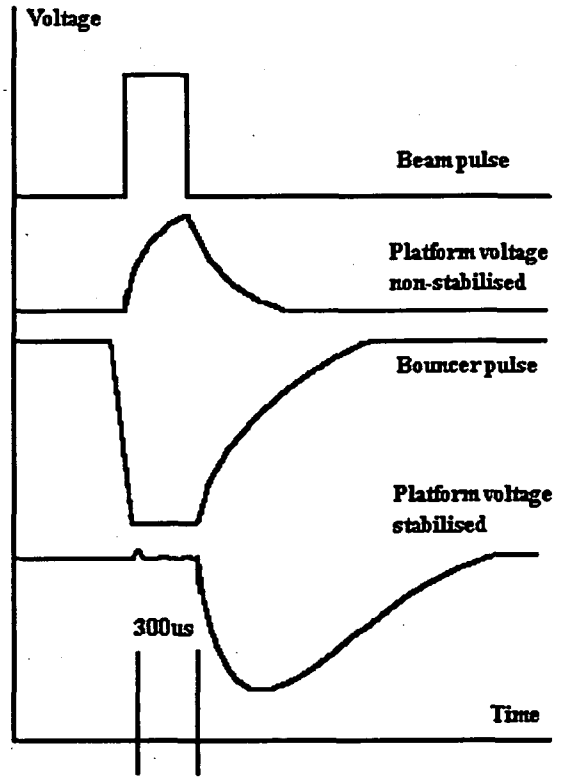

Figure 2 - Platform waveforms

In manual mode, by using feedforward to pre-empt the beam pulse, the natural delays in the circuit can be

overcome to give a better overall stabilisation of the platform voltage.

In automatic mode the present circuit allows adequate stabilisation at the expense of a large negative going overshoot after the beam pulse, as shown in Figure 2. This does not affect the beam stability, but represents wasted power from the pulse amplifier. The maximum voltage swing of 55 kV represents a capability of compensating for beams up to 55 mA, which is well above the normal running current of ISIS.

3.2 Reliability

The operation of ISIS puts great emphasis on both reliability and ease of maintenance. Equipment is expected to perform with extremely high reliability, 24 hours a day for typically 4 week periods. Fault diagnosis is eased by the provision of suitable indication, test points and a signal patching network. All necessary routine maintenance, including valve replacement has been identified and steps have been taken to minimise down-time. Experience has shown the TH5184 gives good service for above 5000 hours. Tubes may be changed in less than 20 minutes and little 'conditioning' is required.

4 FUTURE IMPROVEMENTS

4.1 Control circuit changes

It is intended to develop the control circuitry to introduce a manual/automatic hybrid configuration that will use a gated pulse in conjunction with the beam toroid signal to provide both feedforward and feedback control signals. This should stabilise the platform potential with minimum loss of energy. It should be possible to achieve levels of stabilisation to better than $\pm$ 1 kV both during and after the beam pulse.

4.2 Beam dilution

Beam diluters are fitted to the output of the pre-injector for diagnostic purposes. These are upstream of the beam toroid and so the signal to the Bouncer is reduced. This requires the adjustment of the control loop gain maintain stabilisation of the accelerating voltage. An automatic switching of the gain is to be implemented, allowing the use of the diluter to become transparent as far as the pre-injector is concerned.

4.3 Uprating for larger beam currents

The present design of H^- ion-source has operated for sustained periods at 54 mA. Should future developments of ISIS require the Bouncer to cope with larger currents than this, then it could be uprated using a Thomson TH5186 tetrode. This has "plug-in" compatibility with the TH5184, but has significantly higher performance. An output capacitor with higher working voltage would be required, together with some minor changes to the electronic circuitry.

5 CONCLUSION

The fitting of the higher value current limiting resistor between the high voltage supply and the dc accelerating platform has reduced the effects of column voltage breakdowns and significantly reduced the recovery time after a breakdown. This has significantly improved the availability of ISIS since a breakdown no longer trips the EHT supply and recovery is automatically achieved within a few pulses.

The effects of beam loading of the accelerating voltage resulting from fitting the higher value resistor have been successfully compensated by the design and fitting of a Bouncer system.

6 REFERENCES

[1] Thomson TH5184, Thomson tubes electroniques, 38 rue Vauthier / B.P. 305 / F-92102 Boulogne-Billancourt Cedex / France.

A NEW REMOTE CONTROL AND MONITORING SYSTEM FOR THE ISIS ION SOURCE ON THE 665 KV DC ACCELERATING PLATFORM

M. Perkins, P.J.S.B-Barratt, A.P. Letchford , R. Sidlow, Rutherford Appleton Laboratory, Chilton, Didcot, Oxon, U.K.

ABSTRACT

The control system is based on commercially available equipment and provides a high integrity datalink to the ISIS ion source. The system communicates with the H⁻ source situated at the 665 kV high voltage potential of the DC accelerating column and replaces a 50 Hz 160 bit serial link with a high speed, adaptable, microprocessor based and PC controlled system. The prototype installation highlighted the problems associated with such equipment when used in electrically hostile environments. These have been surmounted with careful consideration to noise immunity and power supply integrity. Software has been written that allows communication between the commercial software and the ISIS (VAX based) control system software. This provides full monitoring and control of the ion source from the ISIS main control room.

1 INTRODUCTION

The performance of the ISIS ion source has improved to an extent where the reliability of the equipment controlling the source is a significant factor.

The ion source is situated on a -665 kV high voltage platform with all its associated power supplies contained within the same Faraday cage. The power supplies both remotely operated and monitored, from the injector control room. Electric mains power at 230 V is supplied by a 6 kVA motor driven alternator.

Electrical breakdowns of the accelerating column make the working environment of any electronics, extremely hostile. The incidence of mains failures is also sufficient to require consideration.

Equipment had previously been controlled using an ISIS designed serial data-link, that presented a 160 bit word, 50 times a second to a decoder to display and control the ion-source parameters. This was linked to the main ISIS control computer by several interface modules. This system was, from experience, overcomplicated and unreliable.

Ion source hardware was undergoing a modernisation so it was decided to up-date the method of control and monitoring of the ion source at the same time.

2 HARDWARE

2.1 Serial link

The heart of the new system is a commercially available, high speed data-link made by Group 3 Technology Limited [1]. This CONTROLNET (tm) consists of a fibre-optic linked 'Device Interface (DI)' that contains a main microprocessor control board and up to three interface boards. These DI's can be daisy chained together for communication to a remotely situated control personal computer (PC). The fibre optic drivers are capable of driving up to 40 metres of plastic fibre. This enabled almost perfect positioning of the control PC in the injector control room.

The installation called for two DI's to be mounted on the EHT platform, Figure 1, with six internal interface boards being selected. These were ;

2 off, 8 channel, configurable analogue input boards,
1 off, 8 channel, configurable analogue output board,
2 off, 24 channel logic input / output boards,
1 off fibre optic RS 232 interface board.

2.2 Digital / analogue interfacing

The RS232 interface was required to connect to a Balzer TPG300 vacuum controller unit. All other equipment was connected via multicore cables. Status and control line were fed on a 19 pole cable to the 5 ion source power supply systems. All analogue set and read signals being made using 2 pole, screened connections.

2.3 Sample and hold

Pulsed signals from the ion source supplies such as, arc current required a sample and hold circuit. This was provided as an 8 channel differential input, and independently timed circuit. All channels are fed to the DI but it also has a multiplexed output to a locally mounted voltmeter, for monitoring purposes.

3 SCREENING

Experience gained from the installation of a prototype system showed that considerable attention had to be paid

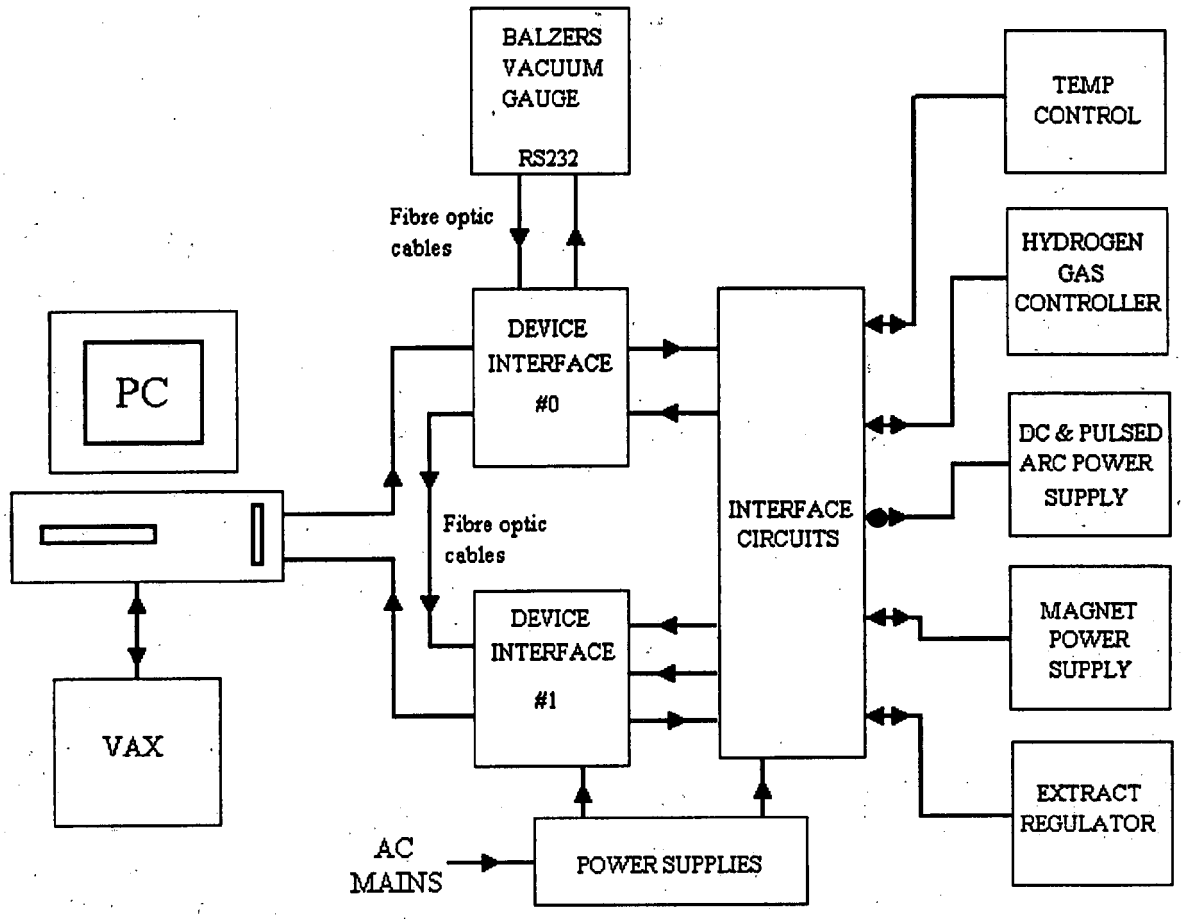

FIGURE 1- BLOCK DIAGRAM OF ION SOURCE CONTROLS

to electro-magnetic noise suppression. Electrical breakdowns had caused both latch-ups of the communication systems and corruption's of the analogue control signals.

3.1 Rf screened enclosure

The most significant step was to mount the entire platform end control system in an earthed, rf screened enclosure. This aluminium box, is mounted on the side of a rack on the EHT platform and has a removable panel with finger strip contacts fitted. No apertures whatever compromise this rf integrity.

All connectors are screened with filtered bulkhead 'D' connectors for status/control signals. The mains input is screened and filtered.

The box contains the power supplies, both DI's, all ferrites, and all interface circuits.

3.2 Ferrite absorbers

At the recommendation of Group 3, ferrite absorbers were fitted to the ribbon cables connecting the DI's to the interface circuits. The fitting of ferrite absorbers to all incoming and outgoing analogue signals was also found to be very successful improvement in immunity against electrical breakdown.

3.3 Printed circuit board

All interface circuits are mounted on one large 350 x 300mm, double layer, ground plane, printed circuit board (pcb). The connections to both analogue and digital grounds are kept separate, following the Group 3 practice. Connections to the pcb are by either ribbon cable or pcb mounting plugs and sockets. A single grounding point is provided for connection to the enclosures' earthing point.

3.4 Power supply integrity

To protect against short-term power supply failures the system is powered from the 230 V ac mains using very basic power supplies with large reservoir capacitance's. This degrades slightly the DI integral power supply versatility but allows the controls to function whilst all around is collapsing. The interface circuits are powered from simple linear power supply modules.

3.5 Firmware

The Group 3 manufacturers were regularly updated the firm-ware with some of the modifications helping the microprocessors to recover from latch-ups. The latest version now allows processor resets and system configuration from the PC and has proved to be successful.

4 PROTECTION

The system is protected from voltage spikes and over-range signals by the use of several different techniques. Most analogue inputs and outputs employ transient absorption diodes and differential π filters. The widespread use of metal oxide varistors has been useful on this and other ISIS pre-injector equipment.

The clamping of set value signals by zener diodes has overcome the upward drift of the set level during a latch-up in communication.

5 SOFTWARE

5.1 Communication

The Group 3 Controlnet contains a dynamic data exchange (DDE) that communicates between DI's and the PC

5.2 Control screen

The control screen and software interface is by a product call INTOUCH by Pantek Ltd. [2]. This is marketed as a man-machine interface and allows generation of the screens for operator control and interfaces the equipment values to the communication software.

5.3 Connection to ISIS controls

The ISIS control system is VAX based and communication is by an ethernet, Local Area Network. The ethernet protocol is Packet Handler for ISIS Data Operations. It was necessary to write software to convert the DDE server protocol to this PHIDO protocol. This is the WinPHIDO packet handler software.

This allows full communication with the ion source from any terminal on the ISIS control network.

6 CONCLUSIONS

The installation of the new ion source datalink and control system has been a major contributor to the reliability of the ion source and hence ISIS. The stability of control and status signals has meant that premature failures of the ion source are rare. The fully installed system has operated for over a year without a single corruption or failure and is being fitted to an ion source test rig for a source development program.

7 REFERENCES

[1] Group 3 Technology Ltd. 2 Charann Place, Avondale, Auckland, New Zealand.
[2] Pantek Ltd, 44 Europa Business park, Bird hall lane, Stockport, UK.

Paper TUP094G submitted for inclusion in the Proceedings of the European Accelerator Conference 1996

HIGH STABILITY OPERATION OF THE ISIS PULSED SPALLATION NEUTRON SOURCE AT 200 μA

C. W. Planner, M. R. Harold, A. I. Borden, P. J. S. Barratt, R. G. Bendall, I. S. K. Gardner, M. Glover, G. H. Rees, D. Wright and C. M. Warsop.
Rutherford Appleton Laboratory, Chilton, Didcot, Oxon, U.K.

ABSTRACT

The ISIS pulsed spallation neutron source now operates with a high intensity of 200 μA. The tuning of such high intensity accelerators is dominated by the successful control and minimisation of beam losses. It is found that there may be a gradual drift in parameter space that limits the synchrotron to a sub-optimal performance. Minimisation of beam loss is critically dependent on the stability of operation of the fast cycling synchrotron, which becomes very sensitive at high intensity, particularly to the intensity and injection conditions. A considerable improvement in stability at 200 μA has been obtained by fitting two new servo systems; one controls the ion source current to stabilise injected intensity and the other controls the synchrotron radial beam position before bunching is complete. Tuning of the synchrotron at high intensity has been simplified by the development of a multiplexing system that allows one pulse in 128 to operate at betatron tunes without tripping on beam loss. This permits fine tuning of the synchrotron whilst operating close to full intensity, before switching all pulses to the new tunes once improvement has been established.

1 INTRODUCTION

The commissioning of ISIS to the full design intensity of 200 μA has been restricted by the limited time available, within the operational requirements for the neutron scattering programme, to control and minimise beam losses for operation at higher intensities. Full intensity was obtained in experimental studies in February 1993 and for a brief period in an operational run in March 1994. For a considerable period subsequent to this it proved extremely difficult to raise the intensity above 180 μA, even in experimental studies. This was eventually shown to be associated with a particular system, adopted operationally, for the minimisation of beam loss.

In the short periods of running at 200 μA it became clear that in order to run consistently at such an intensity, very stable beam conditions were required, particularly at injection and early trapping when space-charge is at a maximum. The ability to fine-tune the synchrotron when operating close to full intensity is also very advantageous. The techniques developed to meet these requirements are described, together with re-tuning methods for the accelerators to obtain very stable operation at 200 μA.

2 TUNING THE ACCELERATORS

Very early in the commissioning of ISIS a set of 'standard settings' was established to minimise the time required to tune the accelerators from start-up. As the intensity was increased and parameters moved to tune for the higher intensity, whilst minimising and controlling beam losses, it became customary procedure to use the final parameters from the previous operational run as the starting parameters for the next. Using this procedure the intensity was gradually increased to 200 μA. The progress to full intensity was dictated by the priority given to the operational neutron scattering programme and the need to establish stable high trapping and acceleration efficiencies at each step with control and minimisation of beam losses. In the synchrotron the lost beam is stopped on specially designed collectors [1] located in approximately one tenth of the circumference

In February 1993 full intensity(2.5×10^{13} ppp) was obtained experimentally and was achieved for a brief period operationally in March 1994. In October 1993 stable operation was obtained at 190 μA, but apart from a brief spell at 200 μA in March 1994, performance fell back gradually to 180 μA and it became very difficult to raise the intensity above this value. It was observed that there were significant changes in the beam profiles in the transfer line from the linac to the synchrotron, but the excitation of the optical elements in the line had not changed significantly. It was thought that this may be due to changes in the ion-source, ion-source optics or the matching from the ion-source to the linac, but after extensive study of historical data no correlation could be found. Eventually a detailed comparison was made of all the accelerator parameters with the settings of October 1993. The most significant differences were the settings for the four linac accelerating cavities' quadrupole and RF parameters. These parameters had been gradually tuned to minimise beam loss in the linac and the RF phases, particularly of cavity 3, had been adjusted to improve trapping in the synchrotron.

Resetting the linac back to the October 1993 parameters restored the profiles in the transfer line to 'normal' and a 200 μA beam was quickly established.

As a result of this experience, the settings for 200 μA are now used at the start of every run. Resetting back to these parameters after any subsequent tuning during the run will ensure that a gradual drift away in parameter space does not occur.

3 STABILISING INJECTED INTENSITY

Operating at full intensity, the fast cycling synchrotron is very sensitive to intensity fluctuations from the linac. These may result from many factors, ion-source stability, space charge neutralisation, optical matching and RF phase and amplitude stability. The ion-source operates with several feed-back systems, but these have limited gain and for historical reasons it is only possible to increment the output in steps of 5 μs. Similar gain limitations apply to the amplitude and phase servo systems for the RF accelerating cavities.

To take account of all possible contributions to intensity fluctuation it was decided to measure the total injected intensity on each beam pulse by integrating the signal from a beam toroid current transformer, just prior to injection. This signal is fed to a comparator amplifier where it is compared with a DC level proportional to the required beam intensity. The output of the comparator is then used to turn off the extraction volts of the ion-source when the set intensity is reached.

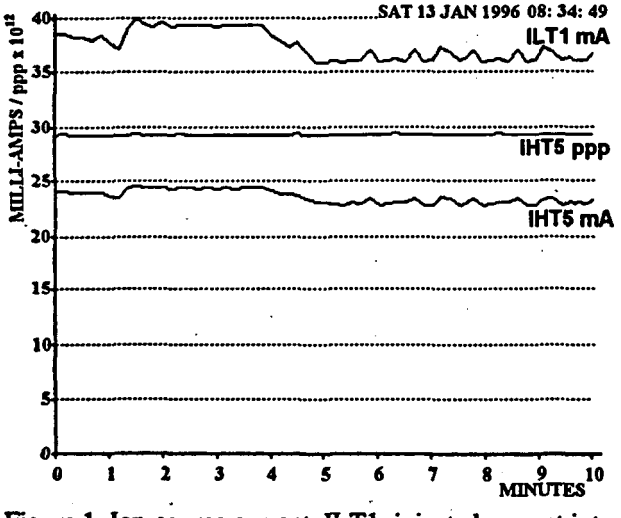

Figure 1. Ion-source current, ILT1, injected current into synchrotron, IHT5, and injected intensity.

The introduction of this servo has improved the injected intensity stability from ±5% to ±0.5%, as shown in Figure 1. In addition, tuning the synchrotron has been made easier by allowing the intensity to be incremented by 0.5% steps instead of ~2.5%.

4 STABILISING EARLY RADIAL POSITION

Though the intensity servo considerably improved the stability at injection there remained some instability, both at injection and the early part of trapping and acceleration, from the synchrotron main dipole field. To keep the beam on its correct radius, a radial servo-loop varies the acceleration frequency to minimise the sum of the non-normalised signals from the ring beam position monitors. Unfortunately these monitors do not give a good signal when the beam is only partially bunched and it was customary to gate the control loop off for the first millisecond or so. During this period any correction to the radial position was applied by adding a fixed "trim function" to the input of the acceleration frequency voltage controlled oscillator. This worked well as long as the synchrotron dipole field remained stable, any field fluctuations at this time could not be tracked and the frequency corrected resulting in radial steering of the orbit and possible beam loss.

To overcome this a programmable function was used as a "demand" signal for the radial loop. The form of this function was determined empirically by finding a value for any given time that was mid way between the limits that would produce beam loss. Once set up it mimicked the non-zero output obtained from the beam position monitors when the beam radius was correct. The use of this function allows the use of the radial loop, during trapping and the early part of acceleration, to maintain a stable radial position for the beam despite fluctuations in the guide field.

5 TUNING ON THE 'FLY'

Tuning of the synchrotron when running at full current, i.e. full intensity and 50 Hz repetition rate, is extremely difficult since any experimental adjustments which cause an increase in beam loss may trip off the accelerator. For this reason the synchrotron is normally tuned with the beam at full intensity, but with the beam pulsing at a sufficiently lower repetition rate so that the beam loss protection can be over-ridden. Starting from a 'standard parameter set' minimises the tuning time, but time at the start of an operational run is always limited. Also, the ion-source performance changes with repetition rate and the performance of other equipment may change as it gradually reaches thermal equilibrium.

To overcome this a multiplexing system has been developed that allows the synchrotron to be tuned experimentally, without tripping on beam loss, whilst running at full intensity and repetition rate. A parallel system of control equipment has been installed for the parameters that are most frequently adjusted:

- Horizontal Steering Dipoles (Horizontal closed orbit)
- Vertical Steering Dipoles (Vertical closed orbit)
- Trim Quadrupoles (Betatron tune Q_H and Q_V)
- Trim Quadrupoles (Harmonic Q-values)
- RF Gap Voltage Function
- RF Frequency Law Trim Function
- Vertical 'Sweeper' Dipole (Controls 'painting' of vertical betatron phase-space at injection)
- Octupole Magnets

Each system can be individually programmed with both a NORMAL and an EXPERIMENTAL set of parameter functions with time. The synchrotron is controlled by the NORMAL functions, whilst the EXPERIMENTAL values can be switched in at a much lower repetition rate. This is usually one pulse in 128, but 1 in 64 and 1 in 32 are available. Adjustments are made only to the EXPERIMENTAL values to study fine tuning of the machine to increase intensity without increasing beam loss to above the trip level.

Tuning in the pulsed experimental mode is carried out by first establishing reference data for the NORMAL function operation. For this mode the total beam loss and intensity signals as a function of time are averaged on a sampling oscilloscope and stored and displayed. The EXPERIMENTAL functions are switched in every 1 pulse in 128 and the oscilloscope is triggered on the same pulse. Tuning can be carried out on this cycle and compared with the reference data, while the affect on machine performance is << 1%. When an improvement is established, the machine can be run initially at 50 Hz on the EXPERIMENTAL values and if satisfactory, these are then transferred to the NORMAL functions.

The success of this method depends to a large extent on the pulse to pulse stability of the beam, since any variations in the 1 in 128 pulse cycle make it difficult to carry out meaningful adjustments. However, the system can now be used successfully for the fine tuning of ISIS at full intensity since the new injected beam intensity servo-system and the greater stability obtained for the early closed orbits have significantly improved the pulse to pulse stability in the synchrotron.

The success of the improvements described culminated with ISIS operating at 200 μA with high stability for the last two operational cycles before the annual long shut-down. For each of the two cycles an average current of 181 μA was obtained for the scheduled running time. The success of the 'standard parameter settings' is illustrated in Figure 2, which shows how quickly 200 μA operation was re-established after the shut-down for the Christmas festivities.

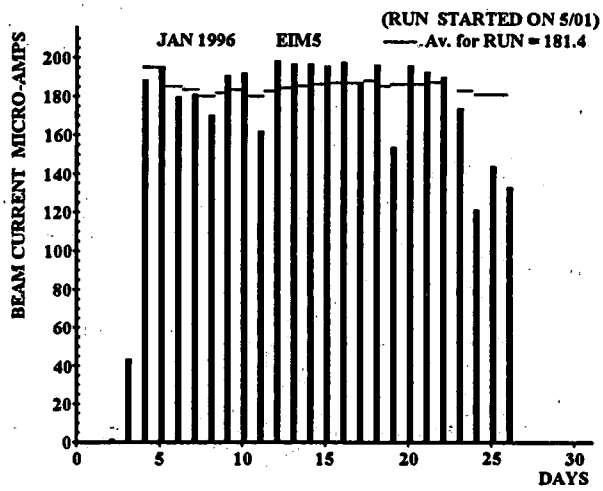

Figure 2. Operational cycle of ISIS running at 200 μA showing average current per day and average current for the cycle

6 CONCLUSION

It has been found that concentration on the control and minimisation of beam loss in high intensity accelerators may lead to a gradual drift in parameter space that can limit the accelerators to sub-optimal performance. As a result, at the start of every operational run, the accelerators are now initially tuned to a particular set of parameters that has been established empirically. Subsequent tuning during the run is allowed, provided reduced beam loss is not at the expense of intensity and an increase in intensity is not accompanied by an unacceptable increase in beam loss.

The development of two servo-systems to stabilise the injected intensity and the radial position during trapping and early acceleration have significantly stabilised the accelerator performance at the full intensity of 200 μA.

The improvement in stability, together with the development of a multiplexing system that allows one pulse in 128 to operate at different tunes without tripping on beam loss, has considerably simplified operations and allowed fine tuning of ISIS when close to full intensity.

REFERENCES

[1] P.E.Gear, BEAM INDUCED RADIATION PROBLEMS AND CURES, this Proceedings.

MULTITURN INJECTION INTO ACCUMULATORS FOR HEAVY ION INERTIAL FUSION

C.R. Prior, Rutherford Appleton Laboratory, Chilton, Didcot, U.K.
H. Schönauer, CERN, Geneva, Switzerland

Abstract

The injection of heavy ions into high current rings is complicated by the unavailability of charge exchange in material foils to produce the singly charged heavy ions needed to keep space charge manageable on the one hand, and because losses need to be rigorously restricted to $\leq 1\%$ on the other.

With these constraints, the number of turns that may be injected by conventional multiturn injection is limited. This paper describes how the number may be increased by a two-dimensional technique of painting Lissajous-like patterns in x–y space, using an inclined or a corner septum. Simulation examples are presented showing the nature of the beam created in the accumulator and the likely effects of space charge forces.

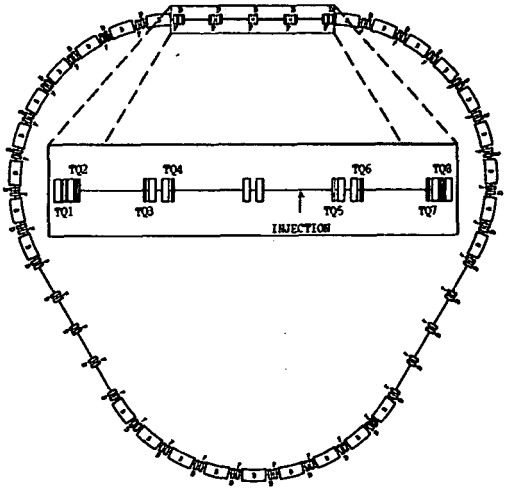

Figure 1: Model accumulator ring for 20 turn transverse injection

1 INTRODUCTION

In the scenarios of a Heavy Ion Driven Inertial Fusion plant (HIDIF) studied to date, singly charged ions from a high current linac are multiturn injected into a number of storage rings before being compressed and merged in the transport to a final focus. At present, a test facility for 10 GeV beam energy delivering 3 MJ within 5 ns to the target is under study [1]. Since the 0.4 A linac pulse in this scenario has a length of the order of 100 km, it is clear that the maximum number of turns that may be injected into each storage ring has a crucial impact on the total circumference and thus on the size and cost of the facility. The injection of 15 or more turns has been attained in operation for decades now; however, efficiencies achieved do not exceed 60%. In order to inject a comparable number of turns with $\leq 1\%$ loss, both transverse dimensions have to be explored. The starting point is the Lissajous pattern of the injected turns in the x–y plane, which is optimised by varying fractional tunes, programming closed orbit bumps and even accumulator lattice functions.

2 MULTITURN INJECTION INTO TRANSVERSE SPACE

For the present study, the aim for transverse space is to inject at least 15 to 20 turns of a beam of singly charged bismuth ions, at 400 mA peak current and $4\pi\mu$m.rad emittance, into an emittance of $50\pi\mu$m.rad in each phase plane. Analysis using an optimising computer code suggests that this can be achieved using an electrostatic septum tilted at an angle $\theta(\sim 60°)$ to the horizontal, which allows both planes to be filled simultaneously. Loss of particles from the circulating beam at the septum is minimised with the correct choice of machine tunes, Q_x and Q_y, allied with the varying closed orbit parameters, x_o, x'_o, y_o and y'_o, at the injection point. Optimum filling of phase space is achieved if the equations

$$\frac{\alpha_{ix}}{\beta_{ix}} = \frac{\alpha_{mx}}{\beta_{mx}} = -\frac{x'_i - x'_o}{x_i - x_o} \quad (1)$$

$$\frac{\alpha_{iy}}{\beta_{iy}} = \frac{\alpha_{my}}{\beta_{my}} = -\frac{y'_i - y'_o}{y_i - y_o} \quad (2)$$

hold, where the subscripts i and m refer to the incoming turn and the accumulator respectively. The injected emittances are then mapped into upright ellipses in the accepting machine's normalised phase space.

Two schemes may be envisaged. In the first, the accumulator parameters, $\beta_{mx}, \alpha_{mx}, \beta_{my}$ and α_{my}, are held constant and only the closed orbit bump varied during injection. Discounting space charge effects, the maximum number of turns that may be injected into the machine without particle loss turns out to be 15 (see table 1). For this model, $Q_x = 8.67, Q_y = 8.78$ and $\theta = 58°$. In the second scheme, the accumulator parameters are varied in such a way that the ratios (1) and (2) are held constant. Little is gained theoretically by varying x_i, x'_i, y_i and y'_i, which would in any case be difficult practically, and x'_o and y'_o are therefore determined directly by x_o and y_o. It is then possible to inject up to 20 turns with $Q_x = 8.62, Q_y = 8.91$ and

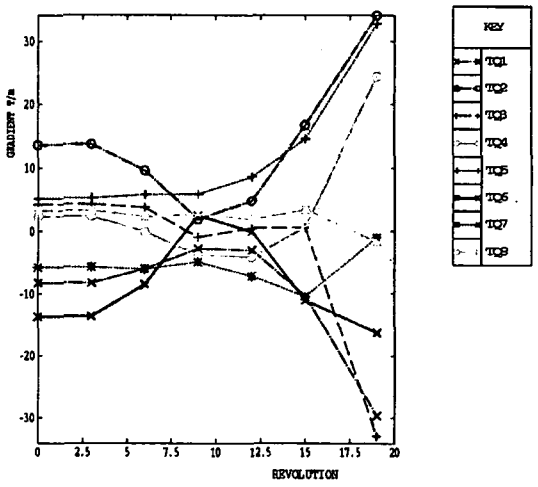

Figure 2: Trim quadrupole gradients for variable–β model

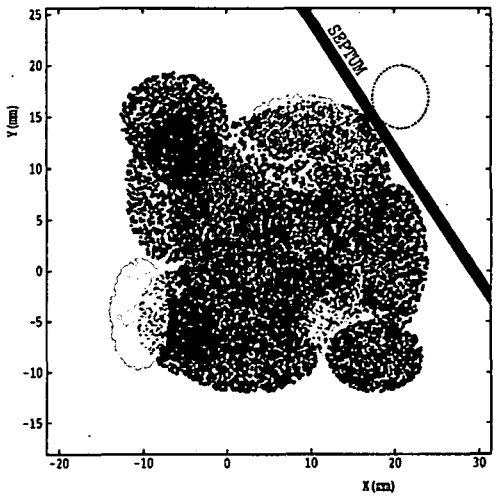

Figure 3: Transverse beam cross section at the end of injection

$\theta = 52.8°$. The optimum model has β_{mx} rising from 4.5 at the start of injection to 8.9 at the end, and β_{my} varying from 5.0 to 8.6 after 7 turns before returning to 5.0 at the end. The closed orbit bump typically falls by 12 mm horizontally but, because of the variation in β_{my}, changes by only 2 mm vertically. Phase space filling ranges from approximately 20 to $50\pi\mu$m.rad horizontally and 38 to $50\pi\mu$m.rad vertically. The vertical phase plane in particular tends to be hollow (see figure 5).

Turns	Loss %	
	fixed β	variable β
≤ 15	0.0	0.0
20	9.94	0.0
25	27.7	5.9
30	42.8	15.5
35	53.1	24.1
40	59.5	31.2
50	69.7	47.1

Table 1. Minimum beam loss for a range of injection turns

Although schemes may be found in which one or two additional turns may be injected without beam loss, in each case the optimised fractional tunes are unsuitable. For the HIDIF scenario under study [1], the values $Q_x = 8.67, Q_y = 8.78$ lie just below the resonance $2Q_y - Q_x = 9$ where there is a reasonable working space. Injection would be into several accumulator rings of the type shown in figure 1. This has superperiodicity 3, which is a design relatively unaffected by instabilities and resonances. The necessary variation in β_{mx} and β_{my}, subject to (1) and (2) and constant tunes, is achieved by means of 8 trim quadrupoles in the injection straight (shown enlarged). The gradients of these quadrupoles (figure 2) are higher than one would prefer and are an obvious drawback of the scheme. However, table 1 highlights the greater possibilities for injection afforded by the variable–β approach, and, since injecting sufficient beam into the required emittance is a major problem, it is likely that further study will concentrate on this method for the immediate future.

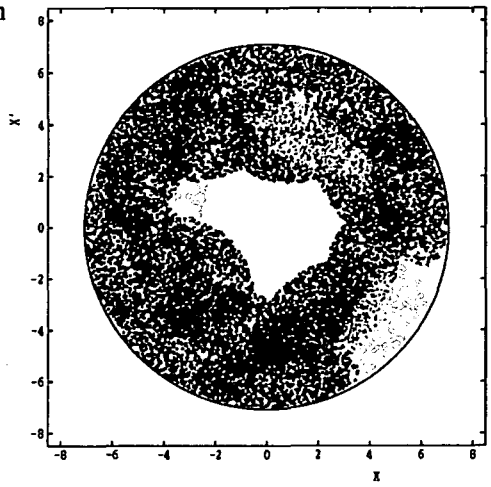

Figure 4: Normalised horizontal phase space at the end of injection

For the 20-turn variable–β model, the layout at the septum in the absence of space charge effects, immediately after the final turn has been fitted into the machine, is shown in figure 3. Figures 4 and 5 show the corresponding projections into each of the normalised phase planes.

The absence of losses in the HIDIF ring, taking into account a likely momentum spread of $\Delta p/p = 2 \times 10^{-4}$ in the linac beam, has been confirmed using the computer tracking code, TRACK2D. This is a development of the code used in an earlier analysis of an optimised injection scheme for HIF, described in [2] and [3]. With space charge taken into account, the tune is depressed by 0.05–0.1, and the re-circulating beam will hit the septum unless the closed orbit scheme is revised. Losses of up to 20% are indicated, based on the same machine parameters. The hollowness in both phase planes is no longer evident and the emittances are increased as individual turns change their alignment. Nevertheless 97% of the injected beam remains within the

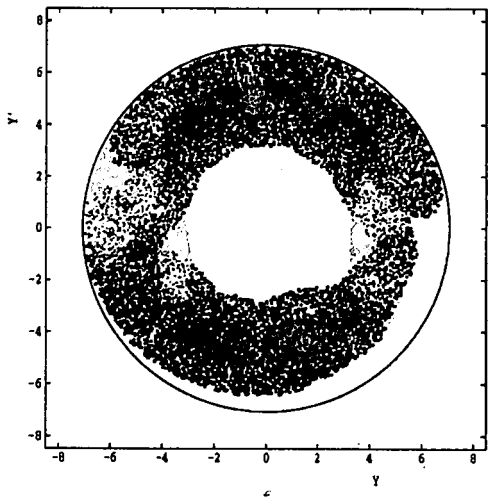

Figure 5: Normalised vertical phase space at the end of injection

required emittances of $50\pi\mu$m.rad, so the halo generated appears quite sparse.

The closed orbit bumps, however, do need to be re-optimised under space charge effects and the indications are that the order of 15–17 turns may conceivably be injected without beam loss by this method. By comparison, the 15-turn fixed–β scheme gives losses under space charge of 16%, suggesting 10–12 lossless turns at best when optimised.

3 ADDITIONAL STACKING IN MOMENTUM SPACE

In view of the limits on the number of turns that may be injected into transverse space, schemes combining betatron stacking with energy ramping and/or RF manipulations have also been investigated. Such injection schemes have been studied for Hadron Facilities like KAON at TRIUMF [4] for thousands of injected turns and, more recently, for heavy ion accumulation in LEAR [5] in the context of the LHC programme. The basic principle is simple: the injection septum is at a place where the normalised dispersion $D_x/\sqrt{\beta_x}$ assumes reasonably large values $\simeq 5\ m^{1/2}$. While the orbit bump removes the circulating beam from the septum, the energy of the incoming linac beam is ramped such that its closed orbit, due to dispersion, remains close to the septum. In the HIDIF scenario this process was imagined as discrete: two or three batches differing by $(\Delta p/p)_{ramp}$ are injected, each one with the optimised procedure of section 2. The amount of this momentum difference is given by

$$\frac{1}{D_x}\left(\frac{2a_x - x + S_x}{\sin\theta} + \Delta x_0\right)$$

where $a_x = \sqrt{\epsilon_{ix}\beta_{ix}}$, S_x is the septum thickness and Δx_0 is the variation of the horizontal bump amplitude during the injection. Both terms are of the order 5×10^{-4}, while the half height of the linac microbunches is now assumed to be 2.5×10^{-4}. After completion of the injection, one is left with two or three ribbons in momentum space. If one injects into stationary buckets at the linac bunch frequency - one RF system per momentum batch - one can merge these ribbons by techniques used in the antiproton production process at CERN [6]. These RF systems also preserve the 400 ns macrobunch structure in the storage rings, in contrast to the barrier bucket system foreseen in the present scenario [1].

However, the scheme, which originally seemed promising, lost its attraction with the development of the estimated parameters of the injected beam: the linac bunch frequency doubled to 216 MHz, the full momentum height increased from 2.5×10^{-4} to 5×10^{-4} and the bunch length from 1.6 ns to 3 ns. In parallel, the target requirements have evolved from 10 ns to 5 ns pulse length; the tolerated momentum spread is still of the order of 10^{-2}. The consequence is simply that there is no space left for stacking in momentum space. In any case, the scheme has to handle the increased space charge forces (keeping the microbunch structure introduces a micro-bunching factor of order 0.45) and the tune variation between momentum batches due to chromaticity.

4 CONCLUSIONS

The analysis therefore indicates that, for the HIDIF study, RF stacking in momentum space is unpromising and the optimal way of injecting sufficient beam is to use a tilted septum and vary not only the closed orbit in both planes but the accumulator lattice functions as well. Further study with particle tracking codes should indicate if the method remains feasible under space charge when the orbits bumps are fully optimised.

5 REFERENCES

[1] I. Hofmann: *Inertial Fusion with Accelerators.* Preceedings of the Fifth European Particle Accelerator Conference, Barcelona, 1996.

[2] C.R. Prior: *Multiturn Injection for Heavy Ion Fusion.* Proceedings of the Symposium on Accelerator Aspects of Heavy Ion Fusion, GSI, Darmstadt, March 1982, p. 290.

[3] C.R. Prior: *Particle Tracking in Solenoid Channels.* AIP Conference Proceedings of the International Symposium on Heavy Ion Fusion, Washington, DC, 1986.

[4] D. Raparia, C.W. Planner, G.H. Mackenzie and J.R. Richardson: *Efficient Capture in an Accumulator of 20,000 Turns of Beam Injected from TRIUMF.* Proceedings of the 1985 Particle Accelerator Conference, Vancouver, IEEE Trans. Nucl. Sci. NS-32, 1985, p. 2456 .

[5] S. Maury and D. Möhl: *Combined Longitudinal and Transverse Multiturn Injection in a Heavy Ion Accumulator Ring,* Internal Note CERN PS/AR/Note 94-12, 1994

[6] D. Boussard and Y. Mizumachi: *Production of Beams with High Line Density by Azimuthal Combination of Bunches in a Synchrotron.* Proc. of the 1979 Particle Accelerator Conference, San Francisco, IEEE Trans. Nucl. Sci. NS-26, 1979, p. 3623.

OPERATIONAL EXPERIENCE OF PENNING H⁻ ION SOURCES AT ISIS.

R Sidlow, P J S Barratt, A P Letchford, M Perkins, C W Planner
ISIS Facility, Rutherford Appleton Laboratory, Chilton, Didcot, Oxfordshire, UK.

ABSTRACT

Over the past eleven years the performance of the Penning H⁻ ion source has kept pace with the development of the ISIS Pulsed Spallation Neutron Source to its current consistent and reliable operation at 200 μA. To maximise the availability of the Spallation Source it has been necessary to develop a number of ion-sources that have a high consistency of performance. These can be changed quickly when ISIS is operational without the need for re-tuning of the high intensity accelerators. Design features of the source to obtain the required output current and duty cycle with an acceptable lifetime are described together with operational experience. Consistent repeatable performance for a number of sources has been achieved by improved refurbishment techniques and quality control.

1 INTRODUCTION

The original development of the H⁻ ion source has been reported earlier [1]. Since then the source has been developed considerably, in line with the development of ISIS.

The source is based on the original Dudnicov design and incorporates a 90° gradient field analysing magnet after extraction with extended pole tips to produce the Penning field for the source. The basic geometry of the Dudnicov discharge region has been retained but the remainder of the design has been changed for ease of manufacture and assembly and to improve performance. The source is mounted separately from the magnet assembly for ease of installation. Design features and operational performance are described together with refurbishing technique.

2 SOURCE DESIGN FEATURES

The source is mounted on the high voltage end of the 665 kV dc medium gradient accelerating column, which forms the pre-injector for the linac. Power supplies and other services are housed on an adjacent high voltage platform inside a Faraday shield.

A schematic diagram of the assembled source is shown in Figure 1. The cathode, anode , aperture plate and extraction electrode are of molybdenum, with the source body and extractor support plate of stainless steel. The cathode is supported in the body by an insulating sleeve of machinable ceramic and is conduction cooled through a copper spacer and 0.6 mm thick mica sheet.

Caesium is supplied from a copper boiler, which houses a 3 gm ampoule of high purity caesium, and is fed to the source through a 6 mm stainless steel transfer line. Two separate heater circuits control the temperatures of boiler and transfer line. The glass ampoule is only cracked once the installed source has been satisfactorily tested.

Hydrogen is supplied via a pulsed piezo-electric gas valve, with the valve pulses regulated to stabilise the mean gas vacuum pressure in the magnet assembly vacuum chamber. Holes in the source body and anode conduct the hydrogen gas and caesium to the discharge region.

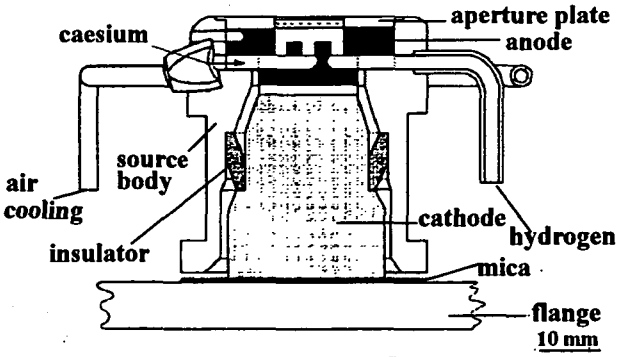

Figure 1. Schematic of ISIS H⁻ ion-source

The poles of the 90° analysing magnet are set into the sides of a stainless steel 'cold box', which is maintained at about −5°C to condense excess caesium emitted from the source. The box is separated from the rest of the magnet iron by a 3 mm gap and the whole assembly operates at extraction voltage. Copper leaf springs connect the cold box to the source extractor and diaphragm plate.

The accelerating column vacuum is de-coupled from the source and magnet assembly chamber by a diaphragm plate that has a 30 mm diameter x 120 mm tube fitted to its centre. The source is pumped by a 2000 l/s turbo pump.

A viewing port allows the extraction gap region and arc discharge to be observed by reflection in the polished surface of the extractor plate. Thermocouples monitor the source anode, cathode and body temperatures.

The ion source arc is fed from two power supplies connected in parallel through diodes. One is a dc supply of 2 A maximum at up to 700 V, the second a current

Table 1. Source Parameters

Source dimensions		units
Cathode to cathode separation	5.0	mm
Anode slot dimensions	10 x 2	mm
Anode thickness	3.5	mm
Aperture slit dimension	10 x .6	mm
Extractor gap	2.3	mm
Source magnetic field :	~0.16	T
Bending magnet :		
Centre gap	25	mm
Angle	90	°
Field gradient (n)	1.0	
Centre magnetic field	0.23	T
Bending radius	80	mm
Diaphragm (source/column) tube aperture (length x diameter)	120 x 30	mm
Typical operating parameters		
Arc current	35-45	A
pulse width	400-650	μs
repetition rate	50	Hz
Extraction Voltage	18	kV
pulse width, typically	230	μs
Typical operating temperatures		
Cathode	490-530	°C
Anode	450-600	°C
Source body	390-460	°C
Cs boiler	165-175	°C
Cs transport Line	300	°C
H^- pulsed beam at 665 keV	35	mA
Normalised emittances at 665 keV		
Horizontal	~180	π mm mr
Vertical	~250	π mm mr

stabilised pulsed supply of 80 A maximum at up to 320 V. The dc supply is used to heat the source to a temperature at which the low impedance, high current, 'caesium mode' discharge may be established.
A list of the main source parameters is given in Table 1

3 SOURCE PREPARATION

There are six operational ion sources and each source is fitted with a new anode, cathode , support insulator and aperture plate. Before assembly all components are first scrubbed and ultrasonically cleaned in detergent, alcohol and acetone and then vacuum baked. After assembly and alignment, the source is tested before storing under vacuum. Testing includes operation of the source in the high impedance mode with hydrogen, using the dc supply at 700 V x 100 mA to establish the integrity of the source and its services.

4 SOURCE OPERATION

After installation on the pre-injector column the source is heated and conditioned to check its integrity by using the dc arc supply, the boiler heating and by pulsing the high voltage extractor. The boiler is then pinched to crack the glass of the caesium ampoule and set initially at 190°C. The arc impedance rapidly falls until it abruptly drops to a very low impedance, 'caesium mode', at which the pulsed arc supply takes over, delivering high current pulses. The dc supply is usually switched off at this point.

Optimisation of the source begins by balancing the power, varying the arc pulse width against the source body air cooling to stabilise cathode and body temperatures. The boiler temperature is then lowered to give stable operation with low noise. A 665 keV H^- beam is then established and further optimisation is done to achieve a 35 mA beam at minimum arc current. Re-optimisation may be required during the life of a source to maintain output.

5 SIGNIFICANT DEVELOPMENTS

Throughout the commissioning of ISIS there has never been the facility to develop the ion source in parallel to operations. Consequently developments occurred in response to the changing demands of the machine on the source performance. The pre-injector was used whenever possible. The developments include equipment external to the ion source but which has a dramatic effect upon its performance, particularly its reliability.

5.1 The Ion Source

A 1 mm deep recess separates the aperture from the plasma to reduce fast electrons. The material to form this was integral to the anode. Over heating caused rapid erosion with a consequent loss of output limiting the useful life of the source to about 14 days. Cooling has been improved by making the material integral with the aperture plate and tightening this down with domed hexagonal headed screws to give extra torque. With this arrangement, erosion is minimal after 27 days of continuous operation.

Cathode temperature is an essential parameter for stable source operation. Monitoring the temperature is difficult because the cathode is at voltage. The problem has been solved by using a thermocouple inside an

aluminium nitride thimble, which is a good electrical insulator but has a high thermal conductivity.

Good source operation depends on the anode temperature being regulated by thermal conduction to the source body. The molybdenum anode fits into two sockets in the body. Improved performance has been obtained by making this an interference press fit to achieve better thermal contact. A more stable source arc has resulted with less anode erosion that has even allowed anodes to be reused.

5.2 EHT Column

EHT column breakdowns create rf fields which have penetrated the shield of the platform enclosure and damaged electronic components or corrupted the control signals. The source arc could be extinguished and recovery would take time and shorten its operational life. Problems associated with this have been considerably reduced by improving the connection between the EHT column and the platform using high power rf finger connection and by improving the noise immunity of the electronic equipment.

5.3 The Bouncer

A Cockroft-Walton EHT generator supplies the -665 kV to the pre-injector column via a 10 MΩ feed resistor, a 0.01 μf reservoir capacitor, and a 10 kΩ resistor linked to the platform. The energy in a column breakdown with this arrangement was considerable. It would damage electronics and switch off the supply on over current.

The 10 kΩ resistor has been replaced by a 1 MΩ resistor and a 'Bouncer'[2] employed to stabilise the platform voltage when the pulsed beam current is accelerated. Column breakdowns are quenched and the platform voltage recovers in less than 60 ms. The effects of the rf fields on ion source electronics has reduced significantly.

5.4 Electrode configuration and aperture tube

The column inner electrode configuration has been changed such that the first two electrodes are a similar conical arrangement to the other 14. They prevent electrons stripped from the H^- beam reaching the glass insulators between the electrodes and charging them until discharge occurs. A reduction in the number of EHT breakdowns ensued.

After changing the first two electrodes there appeared evidence of caesium being deposited from direct line of sight to the source. This has been prevented by fitting a 120 long x 30 mm diameter tube to the diaphragm plate. This had the additional advantage that the column pressure was further reduced resulting in a concomitant reduction in EHT breakdowns. The lens action of the tube to the first electrode did not produce any significant focal effect on the beam at 665 keV.

5.5 Ion source supply filter

The ion source arc discharge produced an oscillation of about 15 MHz which severely affected the two arc power supplies and extracted beam. A π filter and snubber placed immediately after the source stopped the problem.

5.6 Computer Control System

A new computer control system[3] was installed on the platform in 1995. This is based on a commercial PC control system, Group 3 Technology Ltd, New Zealand, supplied by Schaefer Instruments Ltd., Wantage Oxfordshire. The system is susceptible to noise from EHT break downs so considerable care had to be taken to ensure a good noise immune installation. A special applications program, WinPhido, had to be written to enable control via the VAX main computer control system. WinPhido is a DDE (Dynamic Data Exchange) client and server as well as a PHIDO (Packet Handler for ISIS Data Operations) client and server. This system has worked with high reliability and has allowed much tighter control of the ion source parameters. As a result source failures are now rare and they usually reach the end of their life by exhausting the caesium charge. The charge of caesium has been increased by 1 gm to 3 gm which extended the life from 21 to 27 days with no significant increase in source erosion. It is planned to fit a 5 gm charge in the near future with the expectation of extending the source life to include a complete ISIS cycle.

CONCLUSION

A consistent performance is obtained from each of the six operational ion sources due mainly to the quality control of refurbishment and the reliability of the supplies. They each give a stable output of about 35 mA H^- beam at 665 keV and should the lifetime be extended to include a complete ISIS cycle the objectives of the developments will have been achieved.

REFERENCES

[1] P E Gear and R Sidlow, Proc 2nd Int. Conf. Low-energy Ion Beams, Bath, 1980, Inst. Phys. Con. Ser No 54, p284.

[2] M Perkins et al, EPAC 96, MO P 106 G.

[3] M Perkins et al, EPAC 96, TU P 081 L.

CONSOLE OPERATED CONTROL SYSTEM FOR THE RIKEN MUON FACILITY ON ISIS

W A Morris G R Martin S Stoneham *

ISIS FACILITY, CLRC, RUTHERFORD APPLETON LABORATORY, CHILTON, DIDCOT, OXON, OX11 0QX, UK

*ELGOOD & DYE LIMITED

ABSTRACT

An integrated control system for operating the RIKEN/RAL Muon Facility has been completed. The system consists of commercially manufactured equipment and this paper describes: how the communications between them is achieved; the hardware and software architecture from console to field equipment via a Programmable Logic Controller (PLC); the subsequent interfaces to operate power supplies for fast kicker magnets, septum magnets, quadrupole and bending magnets, HV separators, beam slit control and vacuum systems.

1 INTRODUCTION

The following equipment required control and monitoring:

- *Magnets and Power Supplies*

Twenty one Quadrupole; four high voltage Kicker; two Switch Yard; two Septum/Bending and two Crossfield;

- *Vacuum Pumps and control units*

Eight Turbo Molecular Pumps and forepumps, isolation valves;

- *Beam slits and Blockers*

Three slits and four blockers;

- *Machine Interlocks*

Water, Temperature, Vacuum etc;

- *Personnel Interlocks*

Safety, Radiological etc.

The equipment covered an experimental floor area of 500 sq metres and the power supplies were mostly located on a balcony eight meters above the experimental floor.

Controls for the project were seriously discussed in April 1991 and it was recognised that, to operate a facility with a variety of equipment in beamlines and three experimental areas, it could not be done ad hoc.

A RIKEN control room (RCR) was planned in two sections:

a. an air conditioned, experimental diagnostics room with some dedicated controls for superconducting magnets and their refrigeration control system,

b. an experimental data desk top working area for teams of experimenters.

This paper will describe how the operation and control of the facilities power supplies and control equipment was achieved within these constraints.

2 CONTROL PHILOSOPHY AND CONSTRAINTS

It was specified that:

- Control operations e.g., the setting of current and polarity of magnet power supplies, be carried out from the RCR;
- equipment status information, e.g., the position of vacuum line valves, be available from the RCR;
- in case of RCR control failure, equipment should also be capable of being operated locally;
- the control equipment in the RCR could only take up an area equivalent to that of a desk top PC;
- the system needed to be easy to operate with no specialised personnel training.

3 THE CONTROL SYSTEM

The equipment chosen was a Modicon Video Control Panel (console) and Programmable Logic Controller (PLC). This system provided an economical and flexible alternative to hardwired operator control panels. The console could be connected to higher level systems such as host computers and, via the PLC, to lower level functions such as motor and solenoid valve control.

The PLC layout was designed to keep field wiring lengths to a minimum with Input/Output (I/O) modules located in 'drops' distributed around the beamlines.

3.1 *System Configuration*

The control console, sited in the RCR, and the PLC sited in the experimental hall was linked with a twisted shielded pair cable for communications using MODBUS PLUS (an acknowledged *de facto* industry standard communications network).

The console consists of a NEMA 4/12 sealed front panel and membrane keypad able to work in harsh environments.

3.2 *System Layout*

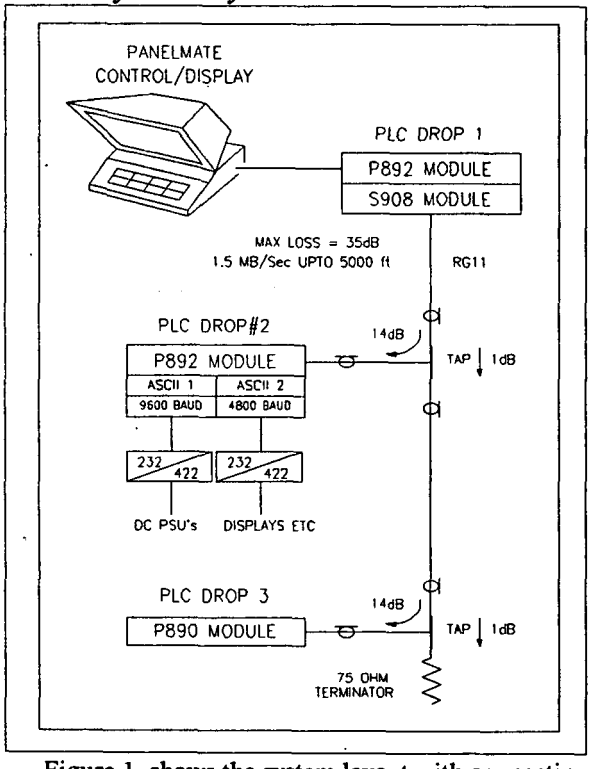

Figure 1. shows the system layout with connecting communications cables.

3.2.1 *Panelmate Plus III (RCR console)*

Users can select and display various screens of templates or graphics from a directory by means of a touch panel, control buttons and numerical keypad.
On screen help messages allow users to rapidly enter and exit relevant pages, to locate sections for display, and carry out on-line operations. A total of 30 pages are available and up to 15 templates per page.

Communication Ports available:
Two RS232 Serial Ports/ Modbus Plus,
One Parallel printer port.

3.2.2 *Programmable Logic Controller (685E)*

The midsized PLC used is a 984-685E (685E) providing large controller power in a modular, expandable architecture. It features 16K words of User Logic and 12.5K words of state RAM (includes storage for 0, 1, 3 and 4XXXX registers) to support 31 Remote I/O drops. A maximum of 1024 discrete I/O points is allowed per drop or can be spread over them all for a total I/O support capacity of 8192 in/8192 out discrete I/O points.. The 685E also supports 9999 registers in 16-bit words.

3.2.3 *I/O Drops and modules*

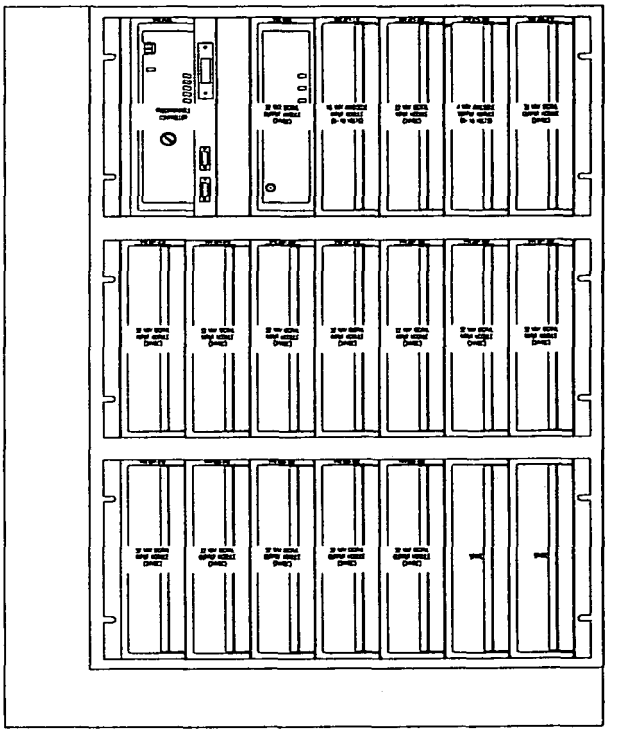

Figure 2. hardware structure of 800 series I/O modules in a 19 inch rack of 7 modules/housing .

Total No of Drops-3

Drop 1 contains the following :

980-685E PLC with CPU and memory.

S908 remote I/O module to communicate with I/O in drop 2 through the P892 interface, and I/O in drop 3 through the P890 interface.

Discrete I/O, 9 input modules/3 output modules
Analogue I/O, 1 input module /1 output module

Drop 2 contain the following:

P892 power module and ASCII comms

Discrete I/O, 5 input modules/2 output modules

Analogue I/O 1 input module

Drop 3 contains the following:

P890 power module

Discrete I/O , 4 input modules/2 output modules

Analogue I/O, 1 input module

Types of I/O modules in the drops:

24V discrete, 32 way input and output,
240V discrete, 16 way output,
0-10V Analogue input and output,
8 way Volt free dry contact.

3.2.4 *ASCII Communications*

Drop 1 PLC module, two ASCII ports are available for communications between dedicated programming devices or PC derived software.

In drop 2 the ASCII ports are used to communicate with power supplies, slit control units and kicker magnet timing modules distributed around the facility as shown in Fig 3.

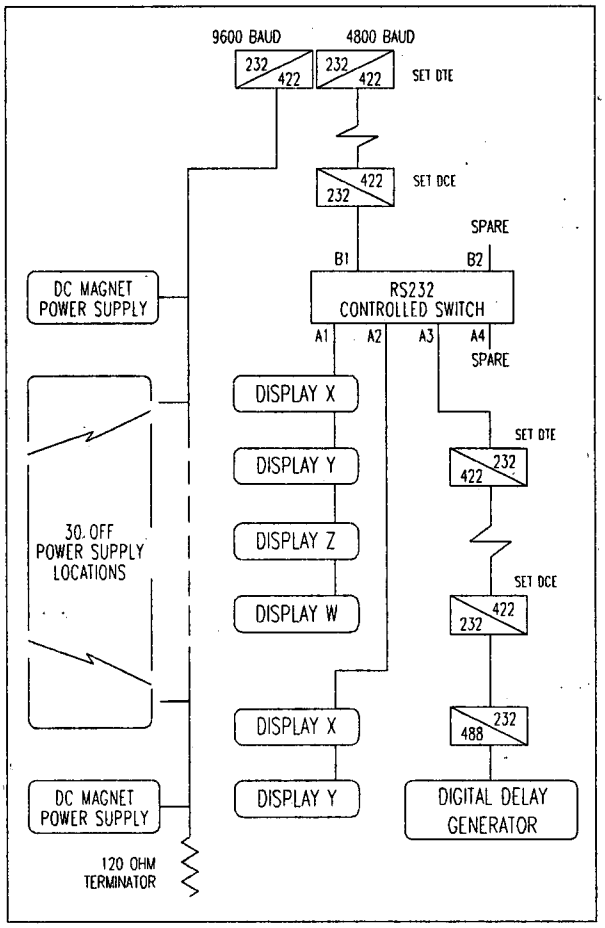

Fig 3. ASCII distribution

Port 1 is set to operate at 9600 Baud and communicates to most of the power supplies. Port 2 is set to 4800 Baud since this is the fastest speed at which the beam slit communications operates.

The RS232 serial comms is converted to RS422 for longer distance operation.
Fifteen of the power supplies were manufactured by Danfysik (Jyllinge, Denmark), most of the remainder are old power supplies with new installed Danfysik control electronics with RS232/RS422 as their standard communications.

The kicker timing generator has IEEE-488 comms with an RS422/IEEE-488 converter interfaces.

3.3 PLC Software

The language used is Ladder Logic and is incorporated in the Modicon Modsoft software package.
Ladder Logic Language is incorporated in a Modsoft software package operating from a laptop PC. The logic is made up of nodes, networks and segments, Fig.4 shows a typical network with contacts and coils.

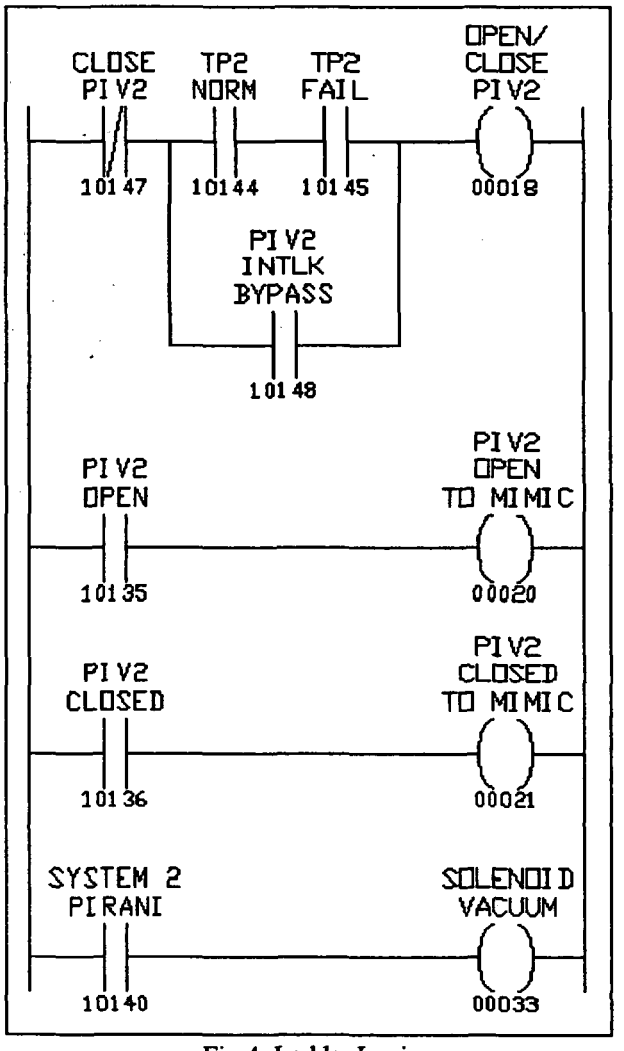

Fig 4. Ladder Logic

Contacts are discrete inputs referenced as 1XXXX numbers and a 32 input module could be referenced 10001 to 10032 inclusive.
Discrete outputs and internal coil contacts are referenced 0XXXX numbers,
Analogue inputs are referenced 3XXXX numbers,
Analogue outputs and internal holding registers are referenced 4XXXX numbers.

A network displayed on the PC screen has seven horizontal lines with up to 11 nodes in a line reading from left to right. The last node(11) on the RHS has to be a coil.
The logic is scanned vertically, down the LHS nodes in the network, then proceeds on the top line to the next node until all nodes are scanned before moving to the next network.
All networks in a segment are scanned before moving to the next segment.
It is possible to choose to miss out a segment during the scan and therefore leave unimportant inputs and outputs to less frequent updating and therefore decrease scan times for essential functions.

The types of nodes are wide and varied from normally open (NO), normally closed (NC), fleeting contacts, coils for output operation, or coils for internal expansion of the ladder logic. The same references can be used as a node many times with the exception of output coils which can only be used once.
Networks can be programmed with counters (up and down) or timing blocks to control the delay of operations.

More specialised blocks are available to carry out mathematical functions of adding, subtracting, multiplication and division.

For example an input analogue 3XXXX reference variable voltage can be subtracted from a constant value and output coils operated if the difference is greater than, less than or equal to the constant.

It is possible to take a register that receives an input or a stored value and transfer it to another register for storage. Conversely it is possible transfer a table of registers of stored values into a single register.

4 CONCLUSIONS

In September 1994 beamline elements were adjusted to run the first muon beam.

At approximately 0900hrs the final beam blocker was opened and after some minor tuning adjustments at 0920hrs muons were observed at experimental port 2. It was originally thought that this first step could have taken several days.

The ease and speed with which this was done amply demonstrates the control and flexibility of the system.